Polariton lasers. Hybrid light–matter lasers without inversion

2012 J. Phys. D: Appl. Phys. 45 313001

(http://iopscience.iop.org/0022-3727/45/31/313001)

J. Phys. D: Appl. Phys. **45** (2012) 409501 (1pp) doi:10.1088/0022-3727/45/40/409501

Corrigendum: Polariton lasers. Hybrid light–matter lasers without inversion

2012 *J. Phys. D: Appl. Phys.* **45** 313001

Daniele Bajoni

Dipartimento di Ingegneria Industriale e dell'Informazione, via Ferrata 1, 27100 Pavia, Italy

E-mail: daniele.bajoni@unipv.it

Received 21 August 2012, in final form 23 August 2012
Published 24 September 2012
Online at stacks.iop.org/JPhysD/45/409501

Reference [115] in the paper refers to the wrong article. The correct reference is Christmann G, Butté R, Feltin E, Mouti A, Stadelmann P A, Castiglia A, Carlin J F and Grandjean N 2008 *Phys. Rev.* B **77** 085310. Reference [115] is cited in the paper in the second paragraph of page 13 and in the captions of figures 11 and 12.

The year of publication of [39] is 2009 and not 2010 as written in the text.

The word 'polaritons' is missing from the sixth sentence of the first paragraph of page 12. The correct phrasing should read as 'In GaAs photonic crystals, surface passivation is very difficult to obtain [4] and a solution has been found, for both interband [5] and intersubband [6] polaritons, by periodically modulating the exponential tail of the photonic part of the polaritons confined in the planar waveguide.' References [4–6] are as in the original published text.

IOP PUBLISHING JOURNAL OF PHYSICS D: APPLIED PHYSICS

J. Phys. D: Appl. Phys. **45** (2012) 313001 (17pp) doi:10.1088/0022-3727/45/31/313001

TOPICAL REVIEW

Polariton lasers. Hybrid light–matter lasers without inversion

Daniele Bajoni

Dipartimento di Ingegneria Industriale e dell'Informazione, Università di Pavia, via Ferrata 1, 27100 Pavia, Italy

E-mail: daniele.bajoni@unipv.it

Received 15 February 2012, in final form 15 May 2012
Published 17 July 2012
Online at stacks.iop.org/JPhysD/45/313001

Abstract

Polariton lasers are coherent emitters in which the fundamental constituents are not photons amplified by a gaining medium but hybrid, part exciton and part photon, quasi-particles named polaritons. In this review we discuss some of the main topics in the field of polariton lasing: we start from an introduction to the concepts of strong coupling regime and polaritons, we then discuss the mechanism of polariton lasing and the main difficulties in achieving it. Some of the main results on polariton lasing reported in the literature, from 2D samples to confined structures, are then reviewed. This latter case will allow us to discuss some of the peculiarities of polariton lasing with respect to traditional lasers. Polariton lasing mostly occurs at cryogenic temperatures, but we will see that it can also be observed at room temperature with a proper choice of materials. To conclude, we will discuss some perspectives for the field.

(Some figures may appear in colour only in the online journal)

1. Introduction

The rapid development of advanced tools and techniques for manipulation, fabrication and characterization of matter at a nanometre length scale is opening new routes towards the efficient control of light propagation and confinement in solid-state materials. As a result, the interaction between semiconductor materials and the confined electromagnetic modes can be considerably enhanced. The ability to integrate semiconductor emitters and cavities to confine the emission has led to a wealth of applications, such as commercially available light-emitting diodes and laser diodes, or to the observation of effects such as the acceleration of the emitter dynamics due to the coupling with the cavity mode (Purcell effect [1]) or the emission of purely nonclassical states of light just to name a few examples.

In the case in which the interaction energy between the emitter and the photon mode becomes larger than their losses, the degeneracy between the emitter and the photon mode is lifted giving rise to two spectrally separated light–matter eigenstates: this regime is called the strong coupling regime. A particular case of strong coupling is that of excitons confined in quantum wells (QWs) and the modes of photonic cavities: the result is hybrid exciton–photon quasi-particles named exciton-polariton (we will refer to them simply as polaritons for the rest of the paper). Polariton lasing is the accumulation of a large population of polaritons in a single quantum state. Polariton lasers have many similarities with conventional lasers, but do not need population inversion to occur: this implies that the polariton lasing threshold is much lower than the photon lasing threshold in a given structure.

In this paper we give an introduction to polariton lasers, and we review some of the main experimental results in the field. The paper is organized as follows: in section 2 we mathematically introduce the concept of strong coupling, giving a definition of polariton and showing how they are mixed states with properties of both photons and matter quasi-particles; in section 3 we describe the mechanism of polariton lasing and we compare it with traditional photon lasing; in section 3.2 we detail the main issues to achieve polariton lasing and in section 4 we show how they have been overcome and we discuss some experimental evidence of polariton lasing in planar samples; in section 5 we discuss how a complete three-dimensional confinement of polaritons can be beneficial for polariton lasing and we take a survey of experimental results of polariton lasing in micropillars and photonic crystal

cavities; we will also see how polariton and photon lasing can be observed and compared in the same sample; in section 6 we briefly review how polariton lasing has been achieved at room temperature in large bandgap semiconductors. Finally, in section 7 we summarize the paper and we discuss some perspectives of the field.

2. The strong coupling regime and the concept of polariton

For most applications the physics of light matter interaction is described to an excellent approximation by the Fermi golden rule [2]. This very general approach can be applied to describe phenomena as diverse as photoluminescence, lasing or scattering of light by particles just to name a few. The regime pictured by the Fermi golden rule is termed weak coupling regime and is a regime of *irreversible* interaction between light and matter; in such a regime the electromagnetic field is either emitted or absorbed by some material resonance (be it for example an atomic transition, a flip between different spin levels of an ion, intersubband or interband transitions in a semiconductor) and then either the material oscillator or the electromagnetic mode dephase before they can interact again. This dephasing may be due to interaction with the environment (for instance a phonon thermal bath in a solid-state systems), or the finite lifetime of the interacting resonances, or escape of photons from the spatial region of overlap with the material resonance.

In the ideal case in which decoherence is absent, the interaction between a single material oscillator and a single mode of the electromagnetic field is characterized by a *reversible* exchange of energy. This regime of electrodynamics is termed strong coupling regime and was firstly postulated by Rabi for nuclear spins in gyrating magnetic fields [3]. The strong coupling regime can be observed in actual systems if the coupling time to the electromagnetic field is faster than all decoherence processes. Strong coupling has been experimentally reported for a wide variety of systems, for example between the modes of high finesse optical cavities and ultra-cold atoms [4], superconducting qubits [5] or single quantum dots [6–8].

In this paper we are interested in the strong coupling regime between excitons confined in a QW and the optical mode of a semiconductor cavity containing the QW (as schematically showed in figure 1(*a*)), firstly observed by Weisbuch *et al* in 1992 [9]. QW excitons are bound states of an electron in the lower conduction band of the semiconductor and a hole in the valence band. In high quality QWs, excitons are well described by a hydrogen atomic model. The state of interest for the internal variable is the 1s orbital, while the centre of mass moves freely in the plane of the QW. For low in-plane wavevectors below the light cone, the dispersion of the exciton energy in phase space can be simply approximated by the kinetic energy of a free particle in the plane of the QW:

$$E_{\mathrm{X}} = E_{\mathrm{X0}} + \frac{\hbar^2 k_{\parallel}^2}{2M_{\mathrm{X}}} \tag{1}$$

where $\boldsymbol{k}_{\parallel}$ is the in-plane wavevector (perpendicular to the growth direction of the QW), E_{X0} is the energy of the exciton for $\boldsymbol{k}_{\parallel} = 0$ and $M_{\mathrm{X}} = m_{\mathrm{e}} + m_{\mathrm{h}}$ is the total mass of the exciton, m_{e} and m_{h} being the electron and hole effective mass, respectively. The material of choice for most applications on QW excitons is GaAs, due to the extremely high-quality QWs that can be obtained in GaAs-based materials by molecular beam epitaxy: in GaAs $m_{\mathrm{e}} = 0.067m_0$ and $m_{\mathrm{h}} = 0.33m_0$ where m_0 is the free electron mass[1]. Being hydrogenoid states, excitons have a well definite binding energy E_{b}, and for temperatures such that $T > \frac{E_{\mathrm{b}}}{k_{\mathrm{B}}}$, where k_{B} is the Boltzmann constant, excitons start to ionize into free electrons and holes; in GaAs E_{b} is around 10 meV, thus excitonic effects in GaAs-based samples are much more relevant at cryogenic temperatures below 100 K than at room temperature.

Excitons are composite bosons: conduction band electrons have spin $\pm\frac{1}{2}$ and valence band holes also have semi-integer spin (in GaAs-based QWs the fundamental exciton is formed with heavy holes, which have spin $\pm\frac{3}{2}$ [10]), so their combination gives rise to particles with integer spin. The fact that excitons follow Bose–Einstein statistics is of fundamental importance for polariton lasing, as further discussed in later sections. The reader can find a complete description of solid-state excitons in the book from Bastard [11]

Semiconductor microcavities are monolithic Fabry–Perot resonators, in which two Bragg mirrors are used to confine light inside a cavity with thickness $L_{\mathrm{cav}} = m * \frac{\lambda}{2}$ where m is an integer [12]. The result is that a standing wave is formed for electromagnetic radiation with wavelength λ inside the semiconductor (termed cavity mode or photon mode from now on). Microcavities conserve translational symmetry in the plane perpendicular to the growth direction so that $\boldsymbol{k}_{\parallel}$ is a good quantum number for the cavity mode which has a definite dispersion. This can be easily calculated considering that, along the growth direction, $k_z = \frac{2\pi}{L_{\mathrm{cav}}}$ so that the energy of the cavity mode is

$$E_{\mathrm{C}} = \frac{\hbar c \boldsymbol{k}}{n} = \frac{\hbar c}{n}\sqrt{\left(\frac{2p\pi}{L_{\mathrm{cav}}}\right)^2 + k_{\parallel}^2} \tag{2}$$

where n is the refactive index of the cavity material and $p \in \mathbb{N}$ is an integer (we will consider only the lowest mode with $p = 1$ in this paper from here on). The cavity mode has a minimum in energy for $\boldsymbol{k}_{\parallel} = 0$, $E_{\mathrm{C,0}} = \frac{2\pi\hbar c}{nL_{\mathrm{cav}}}$. Near the minimum the dispersion is nearly parabolic $E_{\mathrm{C}} \approx E_{\mathrm{C,0}} + \frac{\hbar c k_{\parallel}^2}{2n}$: this implies an effective mass for the cavity mode $M_{\mathrm{C}} = \frac{\hbar n}{cL_{\mathrm{cav}}}$: M_{C} is approximatively four orders of magnitude lighter than M_{X} [13]. A schematic representation of a microcavity is shown in figure 1(*a*): in a typical, GaAs-based sample the cavity has a refractive index larger than the mirrors, has thickness λ and as a consequence the field has a maximum at the centre of the cavity. In actual samples the Bragg mirrors have several tens of pairs to increase their reflectivity and consequently the cavity mode quality factor.

To clearly elucidate the concept of strong coupling between photons and excitons we will apply a simple model

[1] A collection of physical parameters of GaAs can be found at http://www.ioffe.rssi.ru/SVA/NSM/Semicond/InP

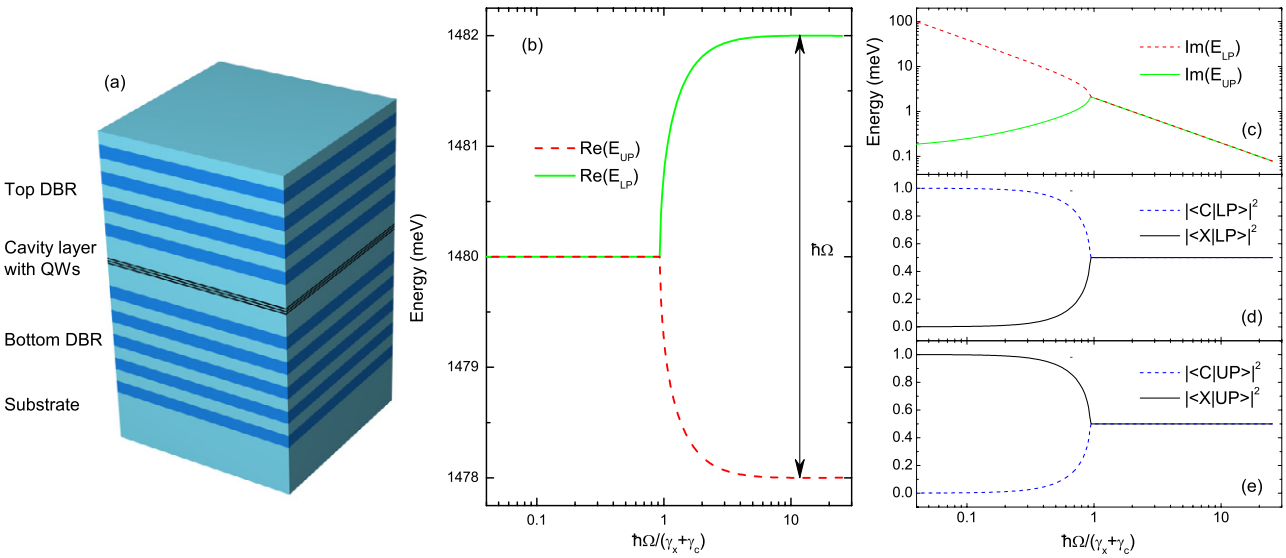

Figure 1. (*a*) A scheme of a semiconductor microcavity. (*b*) The real parts of the eigenmodes obtained from equations (5) using parameters typical for GaAs-based samples ($E_X = E_C = 1480$ meV $\hbar\Omega = 4$ meV) along with (*c*) their imaginary parts and their exciton and photon fractions ((*d*) and (*e*).)

which allows one to calculate the energies of polaritons. The linear optical properties of samples in the strong coupling regime can be easily described using a mathematical picture in which both the exciton and photon resonances are two harmonic oscillators with orthogonal degrees of freedom. In a two dimensional base in which the fundamental vectors are the QW exciton and the photon confined in the cavity (which we will indicate with X and C from now on)

$$|X\rangle = \begin{pmatrix} 1 \\ 0 \end{pmatrix}, \qquad |C\rangle = \begin{pmatrix} 0 \\ 1 \end{pmatrix} \tag{3}$$

the system Hamiltonian can be written in the simple form

$$H = \begin{bmatrix} E_X + i\gamma_X & \frac{\hbar\Omega}{2} \\ \frac{\hbar\Omega}{2} & E_C + i\gamma_C \end{bmatrix}. \tag{4}$$

Here $E - X$ and E_C are the energies of the exciton and photon resonances, γ_X and γ_C their linewidths[2] and $\hbar\Omega$ their coupling [14–16], which we will name Rabi energy. $\gamma_X = \frac{h}{\tau_X}$ where τ_X is the exciton coherence time, mainly due to interaction with the crystalline lattice via scattering with phonons [17, 18], and $\gamma_C = \frac{h}{\tau_C}$ where τ_C is the photon coherence time; this latter is limited by the photon escaping the cavity through one of the mirrors, so is the same as the photon lifetime, and is proportional to the cavity quality factor $Q = \frac{E_C}{\gamma_C} = \frac{E_C \tau_C}{h}$. The coupling is dependent on the oscillator strength of the exciton, the number of QWs contained in the sample and the overlap between the exciton and photon wavefunctions [15].

[2] This model is oversimplified and, as all the simple models described in this review, should be considered for didascalic purposes only. Note in particular that the Hamiltonian of equation (4) is not even Hermitian: the error comes from including the losses within it as imaginary terms, instead of adding the coupling to the continuum of states of the outside radiation field, or to the phonon field, using Langevin terms (as done for example in [15, 38, 56]).

The Hamiltonian of the system can be easily diagonalized yielding new eigenvectors $|\,\mathrm{LP}\rangle$ and $|\,\mathrm{UP}\rangle$ with energies

$$\begin{aligned} E_{LP} &= \tfrac{1}{2}\left(E_X + i\gamma_X + E_C + i\gamma_C\right) \\ &\quad - \tfrac{1}{2}\sqrt{(\hbar\Omega)^2 + (E_X + i\gamma_X - E_C - i\gamma_C)^2}, \\ E_{UP} &= \tfrac{1}{2}\left(E_X + i\gamma_X + E_C + i\gamma_C\right) \\ &\quad + \tfrac{1}{2}\sqrt{(\hbar\Omega)^2 + (E_X + i\gamma_X - E_C - i\gamma_C)^2}. \end{aligned} \tag{5}$$

These new eigenvectors are called polaritons: the lower polariton $|\,\mathrm{LP}\rangle$ and the upper polariton $|\,\mathrm{UP}\rangle$. Note that the exciton and photon energies are dependent on the parallel wavevector through equations (1) and (2), but we have dropped in equation (4) and (5) the explicit dependences for sake of clarity.

Let us now, for a moment, consider the eigenvalues and the eigenvectors at fixed $k_\parallel$ (typically $k_\parallel = 0$). Figures 1(*b*) and (*c*) show the real and the imaginary parts of the energies of equations (5) while varying the ratio $\frac{\hbar\Omega}{\gamma_X+\gamma_C}$. We have taken $E_X = E_C = 1480$ meV and $\hbar\Omega = 4$ meV, which are typical values for a GaAs-based sample containing InGaAs QWs. While for $\hbar\Omega < \gamma_X + \gamma_C$ the energies of the system's resonances remain unchanged with respect to the case of no coupling, when $\hbar\Omega > \gamma_X + \gamma_C$, a drastic change in the energies and the eigenvalues occurs as they split into two distinct eigenvalues. The condition $\hbar\Omega > \gamma_X + \gamma_C$ corresponds to the situation in which the interaction between the two fundamental oscillators is faster than their decoherence time, and thus the interaction becomes reversible, and is called the *strong coupling regime*, in contrast with the weak coupling regime given by $\hbar\Omega < \gamma_X + \gamma_C$. A lot of insight into polariton physics can be gained by considering the square moduli of the projections of the new eigenstates on the photon and exciton states:

$$\begin{aligned} \alpha_{LP} &= |\langle C \mid \mathrm{LP}\rangle|^2, & \beta_{LP} &= |\langle X \mid \mathrm{LP}\rangle|^2 \\ \alpha_{UP} &= |\langle C \mid \mathrm{UP}\rangle|^2, & \beta_{UP} &= |\langle X \mid \mathrm{UP}\rangle|^2 \end{aligned} \tag{6}$$

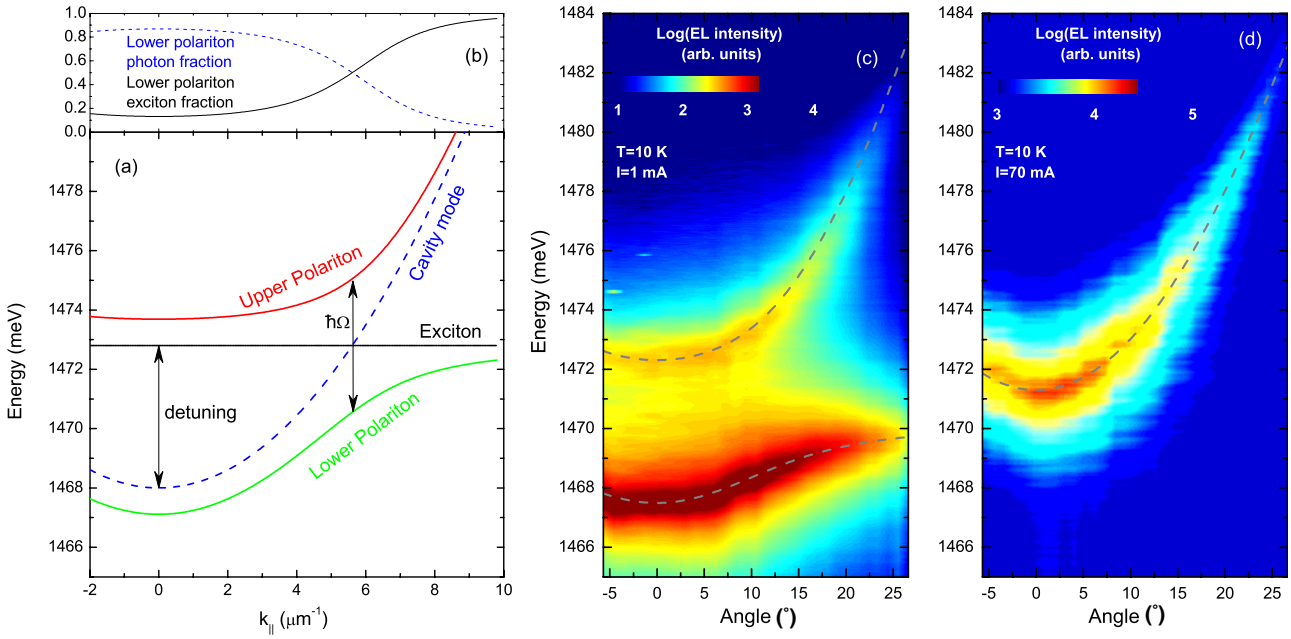

Figure 2. (*a*) Dispersion of the polariton branch calculated for the sample of [138] and (*b*) the photon and exciton fractions of the lower polariton branch. Electroluminescence spectra showing the dispersion of the emission in the case of (*c*) strong coupling (at low pumping rate) and (*d*) weak coupling (at high pumping rate). The data of (*c*) and (*d*) are taken from [138], the experiments are performed at a temperature of 10 K and the emission intensity is in log scale. The dashed lines indicate the calculated polariton dispersions in (*c*) and the photon dispersion in (*d*)).

α_{LP} (α_{UP}) is called the photon fraction of the lower (upper) polariton, while β_{LP} (β_{UP}) is called the exciton fraction of the lower (upper) polariton. These quantities are plotted in figures 1(*d*) and (*e*): in the weak coupling regime, the eigenmodes of the system remain completely photon and completely exciton, while in strong coupling $|\,\mathrm{LP}\rangle$ and $|\,\mathrm{UP}\rangle$ have nonzero projection on both $|\,P\rangle$ and $|\,X\rangle$. Polaritons are therefore hybrid states, part exciton and part photon (sometimes called dressed states [19]). The behaviour of polaritons, detailed in the following sections, can be often explained in terms of a superposition of exciton and photon properties, weighted with the respective fractions $\alpha_{\mathrm{LP,UP}}$ and $\beta_{\mathrm{LP,UP}}$. In particular, polariton's lifetimes and effective masses are given by

$$\begin{aligned}\frac{1}{\tau_{\mathrm{LP,UP}}} &= \frac{\alpha_{\mathrm{LP,UP}}}{\tau_{\mathrm{C}}} + \frac{\beta_{\mathrm{LP,UP}}}{\tau_{\mathrm{X}}}\\ \frac{1}{m_{\mathrm{LP,UP}}} &= \frac{\alpha_{\mathrm{LP,UP}}}{m_{\mathrm{C}}} + \frac{\beta_{\mathrm{LP,UP}}}{M_{\mathrm{X}}}.\end{aligned} \tag{7}$$

The photonic part of polaritons accounts for their low mass and density of states, and their coupling to the external radiation field. Their excitonic part gives them the ability to interact with the lattice through phonon scattering, self-interaction through dipole–dipole and hopping potential and sensitivity to external electrical fields.

In the general case the energies of the polaritons, their photon or exciton fractions as well as their lifetimes are all dependent on the in-plane wavevector. This dependence can be easily obtained by explicitly inserting the dependence on $k_{\parallel}$ of the exciton and photon modes in the Hamiltonian of equation (4). Figure 2 (*a*) shows the dispersion of exciton polaritons in phase space for a typical sample (calculated using equations (5)) along with the dispersion of the exciton and photon modes in weak coupling. The lower polariton branch has a peculiar, s-shaped curve, with a minimum at centre of the Brillouin zone at $k_{\parallel} = 0$ while it tends asymptotically to the exciton energy at large wavevectors. Two fundamental quantities are marked in the figure: the Rabi energy $\hbar\Omega$ and the detuning, defined as $\delta = E_{\mathrm{C}}(k_{\parallel} = 0) - E_{\mathrm{X}}(k_{\parallel} = 0)$. The dispersion of polaritons can be measured in angle-resolved experiments, as the wavevector can be linked to the observation angle ϑ by

$$k_{\parallel} = \frac{\omega}{c}\sin(\vartheta) \tag{8}$$

where $\vartheta = 0$ is the direction perpendicular to the sample surface (growth direction). An example of experimental polariton luminescence is shown in figure 2(*c*): both the dispersion of lower and upper polariton branches are clearly visible, well in accord with the calculated dispersions of figure 2(*a*). The exciton and photon fractions of the lower polariton branch are shown in figure 2(*b*): the states around the energy minimum (sometimes called polariton trap) are strongly photonic, while the states at high $K_{\parallel}$ are mostly excitonic. We will see in the next session that these properties of the lower polariton branch play a fundamental role in polariton lasing.

3. Polariton lasing

Polariton lasing was firstly proposed in a theoretical paper by Imamoglu *et al* 1996 [20]. Figure 3 shows a scheme of the polariton lasing mechanism in a two-dimensional semiconductor microcavity: the sample is excited non-resonantly, high above the QW levels, typically through an

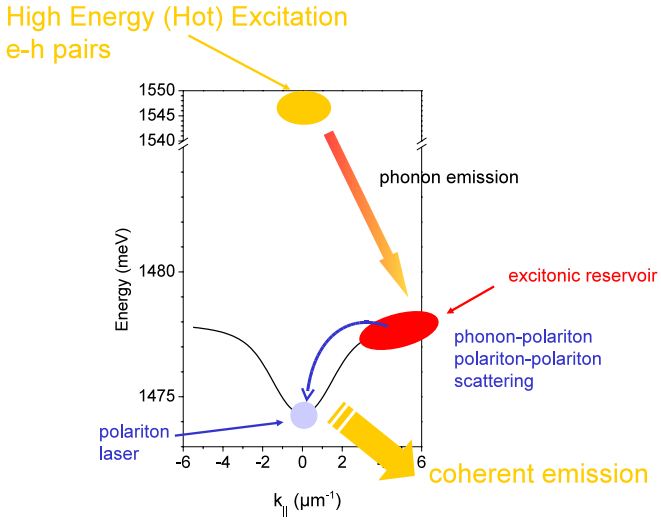

Figure 3. A schematic representation of the mechanisms involved in polariton lasing: the black curve represents the lower polariton branch.

optical pump, continuous wave or pulsed. The pump creates a plasma of electron hole pairs which subsequently lose energy through the emission of phonons [21]. As the carriers relax, they start to occupy the polariton states in the excitonic reservoir and then, by emission of phonons or some other relaxation mechanism (see sections 3.2 and 4) they should relax further down to the lower polariton branch. This process eventually comes to an end when the minimum of the lower branch at $\boldsymbol{k}_{\parallel} = 0$ is reached: this state is, at least in principle, privileged for the accumulation of polaritons and consequently for polariton lasing. Let us name $\mathcal{R}_0^{k,0}$ the probability of a polariton to relax from a state of wavevector $\boldsymbol{k}$ to $\boldsymbol{k}_{\parallel} = 0$ when this latter state is empty. The term $\mathcal{R}_0^{k,0}$ was theoretically studied by Tassone and linked to the interaction with the lattice [22]. When accounting for the mean population $\langle N_0 \rangle$ in the energy minimum, the scattering rate becomes

$$\mathcal{R}^{k,0} = \mathcal{R}_0^{k,0} \left(1 + \langle N_0 \rangle\right). \tag{9}$$

Polaritons are dressed states of two bosonic particles, excitons and photons, and have therefore integer spin and follow the Bose–Einstein statics. One of the basic properties of bosons is that the scattering rate towards a final state is proportional to the population to the state plus one [2, 19]. The idea underlying polariton lasing is that, if the mean occupation factor $\langle N_0 \rangle$ exceeds unity, then scattering towards the state at $\boldsymbol{k}_{\parallel} = 0$ becomes increasingly favoured with respect to every other state. This positive feedback thus entails the formation of a macroscopic population of polaritons in the final state: the higher $\langle N_0 \rangle$, the more efficient is the scattering rate described by equation (9) and so on. There is a 'population threshold' at which the final state population is expected to increase exponentially by several orders of magnitude by increasing the pumping power. This behaviour is similar to what observed for a conventional laser, in which the threshold is reached when the photon occupancy for one of the cavity modes reaches unity, and the emission from the gain medium is concentrated to that mode [12]. Just as in the case of the classical laser, the term proportional to the final population in equation (9) comes from the properties of bosonic commutators [19]: once $\langle N_0 \rangle > 1$ the phase of polaritons scattering towards $\boldsymbol{k}_{\parallel} = 0$ is locked to the phase of those already occupying the final state. This in turn means that the threshold is associated with an increase in temporal coherence for polaritons, measurable as line narrowing or an increase in the first order Glauber coherence [23]: a further analogy with the polariton laser. The same analogy holds for the second order degree of coherence $g^2(\tau = 0)$ [23]: it has been calculated [24], and measured [25, 26], that at threshold the value $g^2(\tau = 0)$ passes from a value >1 (meaning that the polariton population has thermal temporal statics [19]) to a value of $g^2(\tau = 0) = 1$ (meaning that the polariton population has Poissonian temporal statics [19]).

A further similarity between polariton and photon lasing comes from the fact that, in a typical experiment, the system is studied by observing the light escaping through the mirror: as we have seen in section 2 polaritons mainly decay radiatively through their photonic component. The escaping photons bear the properties of the emitting polaritons: polariton lasers are thus observed as sources of bright coherent beams of light.

These analogies between the relaxation of polaritons amplified by final state occupancy and a classical laser have led to the term 'polariton laser' to describe the phenomenon. The term is not completely correct: the basic physics of the system is indeed stimulated relaxation of quasi-particles, and not 'stimulated emission of radiation'. There are nonetheless several properties that make polariton lasers different from their conventional counterparts, some of which will be discussed in section 5.

One such difference pertains the level of excitation (i.e. the pump power) the sample needs to reach polariton lasing. As we have seen in section 2 excitons are two-particle wavefunctions of electron and holes of semiconductors bound to form a hydrogen-like bound state. This picture is, however, only accurate if the conduction and valence bands are almost empty: electrons and holes are in fact fermions and can occupy only one state in phase space each. Increasing the pumping of the sample means increasing the number of electron and holes injected in the bands: as the conduction and valence bands are filled, fewer and fewer 'free' states are available to build the two-particle wavefunction of the exciton. This phenomenon is known as phase space filling [27, 28], and gives rise to a decrease in the exciton oscillator strength [29] and thus a decrease in $\hbar\Omega$ in equation (4): at high pumping powers there is a gradual loss of coupling strength between the exciton and photons. Eventually, when the bottom of the conduction and valence bands is completely filled, no excitons can exist in the system anymore, and so no polaritons as well: this transition is called the Mott transition, and occurs in GaAs-based QWs for injected densities of electron hole pairs around 10^{11} cm^{-2} [30]: above the Mott transition no strong coupling is possible (an example of transition to weak coupling due to excessive pumping is shown in figure 2(*d*)), let alone polariton lasing. On the other hand the complete filling of the bottom of the conduction and valence bands is necessary to obtain classical gain in the QW, and classical photon lasing in the

sample [31]. This means that the threshold for polariton lasing necessarily occurs at lower pumping power than the threshold for classical lasing in the same sample.

Note that the picture described above, of gain due to stimulated relaxation of particles that are partly excitons, may not be limited to the strong coupling regime. The simple model described in section 2 allows for a limited admixture of states even if the losses exceed the coupling; in this picture the eigenmodes of the system are photons with a weak excitonic character, and vice versa. As an example, some indication of excitonic gain without Rabi splitting has been recently shown in a ZnO-based cavity [122]. However, for simplicity, in this paper we will describe polariton lasing only within the framework of the strong coupling regime, the regime in which the concept of polariton as described in section 2 is fully relevant.

3.1. A brief note on polariton lasing and polariton condensation

Soon after the first experiments showing the occurrence of strong coupling between excitons and photons in semiconductor microcavities, polaritons appeared to be excellent candidates for the observation of Bose–Einstein condensation in a solid-state system. Condensation had already been sought for QW excitons but had not been observed because of exciton decoherence due to scattering with phonons, and has only recently been experimentally observed [32–36]. Polaritons have several advantages with respect to excitons. Owing to their steep dispersion relation (much steeper than excitons, as discussed in section 2), they have a much lower mass than the exciton. If we consider a general two-dimensional gas of particles or quasi-particles, quantum degeneracy is achieved when the mean separation between the particles is shorter than their de Broglie wavelength $\lambda_{\mathrm{DB}} = \frac{2\pi}{k}$ (k being the module of the particle wavevector [2]), so that the wavefuctions overlap and indistinguishability becomes relevant [37]. This translates to

$$\sqrt{n}\lambda_{\mathrm{DB}} \geqslant 1 \tag{10}$$

where n is the two-dimensional density of the quasi-particles. If we consider the gas to be thermalized, and the quasi-particles to obey a 'free particle' parabolic dispersion with effective mass M, we can write the energy as $\frac{(\hbar k)^2}{2M} = k_{\mathrm{B}}T$, where k_{B} is the Boltzmann constant and T is the temperature. Hence, equation (10) becomes

$$\frac{n}{k_{\mathrm{B}}T} \geqslant \frac{2M}{h^2}. \tag{11}$$

The lighter the mass of the quasi-particle the easier it is to achieve condensation (lower densities or higher temperatures). The lower effective mass of polaritons with respect to excitons makes them excellent candidates for the observation of condensation: imposing a density $n = 10^9$ cm^{-2} in equation (11) one obtains a temperature of about 20 K for polaritons, in contrast to tens of mK for excitons [38, 39][3].

[3] This kind of calculation is of course oversimplified: the reader can find a correct theoretical estimation of the critical temperature for polariton condensation in several materials in [38] and an experimental study of polariton lasing thresholds from 4 K to room temperature in a GaN sample in [39].

Following these reasons the observation of bosonic stimulation for polaritons and spontaneous formation of a coherent macroscopic polariton population have been interpreted as polariton Bose–Einstein condensation [40–42]. This interpretation is further backed by the properties that coherent polariton gases have in common with atomic condensates [43] (as briefly mentioned in the conclusion of this paper). The phenomenon of polariton condensation is exactly equivalent to the polariton lasing we have described in the previous section, and further investigation showed that thermal equilibrium is not achieved by the polariton gas, so that the term Bose–Einstein condensate is not exact and a weaker definition of condensation, which does not involve thermal equilibrium, has been applied to the justify the term condensation for polaritons [44]. Neither the term 'polariton laser' nor 'polariton condensate' is therefore completely correct, and the debate on the nature of the phenomenon is still open: the issue has been, for example, recently addressed in the letter of Butov and Kavokin to Nature Photonics [45] and in the response of Deveaud-Plédran [46].

In this paper we will use the term polariton laser for coherent polariton ensembles, but the reader should not find it ambiguous if we refer to theoretical and experimental works on polariton condensates as well: the terms 'polariton laser' and 'polariton condensate' can largely be considered synonymous.

3.2. The difficult way through the bottleneck

More than a decade passed between the first observation of microcavity polaritons and that of polariton lasing. The main problem is that the polariton gas is an open system, as polaritons can decay radiatively with a time which decreases as their photonic component increases as seen in equation (7). The polariton laser is therefore a dynamical system, in which the final state population must be created and maintained against its natural decay via recombination of its excitonic part. Let us limit ourselves, for the moment, to relaxation of polaritons by the emission of acoustic phonons, the main relaxation process at low pumping powers. The process of phonon emission is elastic, so that both the energy and momentum of the emitted phonon must match the loss in energy and momentum of the relaxing polariton:

$$\begin{aligned} E_{\mathrm{ph}}(\mathrm{k}_{\parallel,\mathrm{ph}}) &= E_{\mathrm{LP}}(\boldsymbol{k}_{\parallel,i}) - E_{\mathrm{LP}}(\boldsymbol{k}_{\parallel,f}), \\ \boldsymbol{k}_{\parallel,\mathrm{ph}} &= \boldsymbol{k}_{\parallel,f} - \boldsymbol{k}_{\parallel,i} \end{aligned} \tag{12}$$

where $\boldsymbol{k}_{\parallel,\mathrm{ph}}$ is the in-plane component of the phonon wavevector. Polaritons do not have a well-defined wavevector along the growth axis z of the sample: the cavity structure is not translationally invariant along z, so there is no momentum conservation, and thus emitted phonons can have an arbitrary component q_z and polaritons can relax towards a continuum of final states. There is, however, a limiting value to q_z as well, given by the QW thickness L_{qw}: the probability of emitting a phonon lowers exponentially for $q_z > \frac{2\pi}{L_{\mathrm{qw}}}$. The dispersion of acoustic phonons is very different from the polariton dispersion, the former being almost flat on an energy scale as that of figure 2(*a*) [47]. Combining the limit on q_z with

equation (12) and the phonon dispersion curves in GaAs (see footnote 1) one obtains that the maximum energy a polariton can lose with a single phonon emission is less than 2 meV.

The result is that polaritons cannot directly relax from the excitonic reservoir to the minimum at $k_{\parallel} = 0$, but they need to emit a large number of acoustic phonons losing a small amount of energy each time, gradually leaping down the lower polariton branch. Unfortunately, the more they relax towards the minimum the more their photon fraction increases (see section 2 and figure 2(*b*)): the hybrid nature of polaritons is detrimental when it comes to relaxation. On the one hand, the process of scattering with phonons is proportional to the exitonic part [48]: the more photonic the polaritons become, the less likely will be their interaction with the lattice and longer delays will pass until the next relaxation step. On the other hand, following equation (7), the radiative lifetime of polaritons considerably decreases with increasing their photon fraction. The net result is that polaritons are more likely to radiatively decay during the process of relaxation towards the energy minimum before actually reaching the minimum. This effect is called the relaxation bottleneck, and has been experimentally reported in several samples [22, 49–51]. An example of bottleneck effect is shown in figure 4: a microcavity sample is pumped non-resonantly, and the resulting photoluminescence is shown as a function of energy and wavevector. The profile of the lower polariton band is clearly visible, but the maximum of the emitted intensity is not found in the energy minimum, but at higher wavevector states (around an angle of 15–20° in the figure).

The bottleneck effect has hindered the observation of polariton lasing: because of it, a population of unity could not be achieved in the polariton trap for pumping powers below the Mott transition and the loss of strong coupling in the sample. Several ways have been tried to overcome the bottleneck effect, including cavities designed to harness the much more efficient optical phonons instead of acoustic phonons for relaxation [52] or the injection of an electron gas in the QW to achieve electron–polariton relaxation [53–55]. We will see in the next section that the solution has been found improving the cavity design and quality.

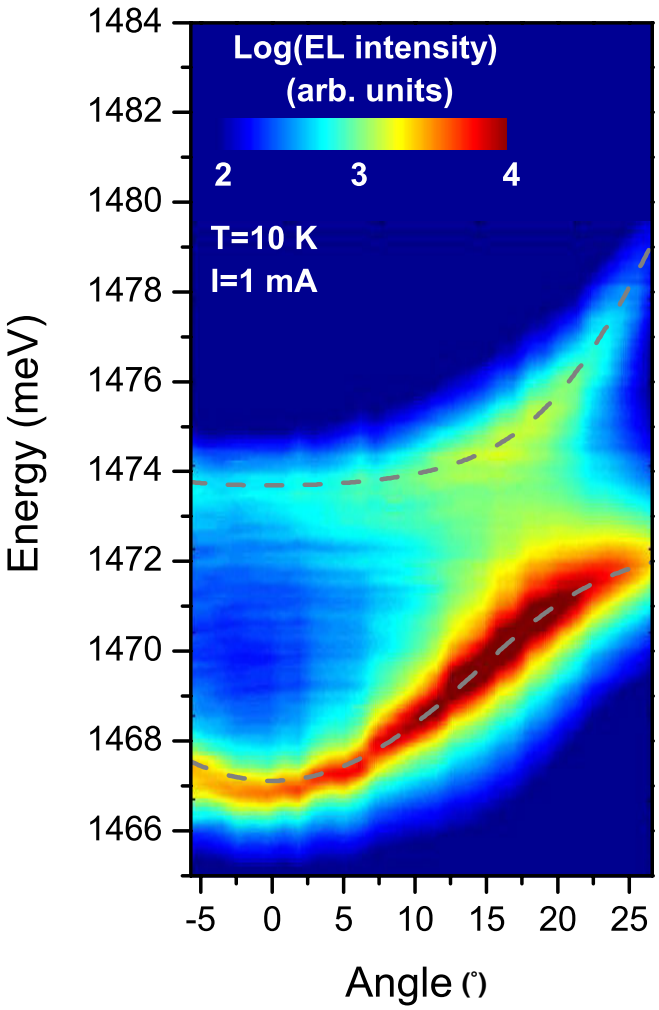

Figure 4. Electroluminescence spectra showing an instance of relaxation bottleneck: the emission is stronger at high angles while the energy minimum of the lower polariton branch remains scarcely populated. The data are taken from [138], the experiments are performed at a temperature of 10 K and the emission intensity is in log scale.

4. Polariton lasing in planar structures

The first instances of polariton lasing were reported in two-dimensional microcavity samples such as those described in section 2. The problems associated with the bottleneck described in the previous section have been solved combining two strategies related to the design and realization of the samples.

The first was to increase as much as possible the quality factor of the photonic mode of the microcavities. As we have seen in the previous section, one of the limiting factors for achieving polariton lasing comes from radiative recombination of polaritons when they relax towards the trap at $\boldsymbol{k}_{\parallel} = 0$, owing to their increasing photonic fraction. In turn, the radiative recombination time is directly proportional to the quality factor of the cavity. As a result, doubling the latter means doubling the lifetime of polaritons in the trap, and hence doubling their population at a given pump power. The increase in the quality factor of microcavity samples has been due to steady improvements in growth techniques allowing the realization of Bragg mirrors containing more than 30 pairs: samples with photon lifetimes of the order of several picoseconds are currently available.

The second approach consisted in increasing as much as possible the number of QWs contained in the samples. The rationale for this choice is that the total density of excitons is limited by the Mott transition to some 10^{10} cm^{-2} per *each* QW. This limit does not hold for polaritons. Being hybrid states of excitons and photons, they are spatially distributed along the profile of the photon mode. If this latter encompasses more than one QW, then strong coupling is achieved between photons and excitons in each of the QWs. This means that, if the sample contains ten QWs, then the maximum number of injected polaritons increases by an order of magnitude with respect to the maximum number of excitons that can be injected in one QW. The difficulty in this approach is that, to

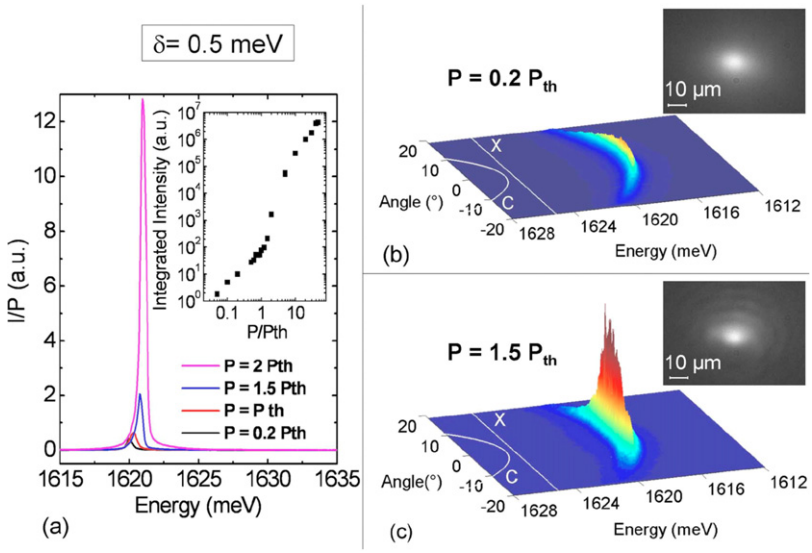

Figure 5. An instance of polariton lasing in a 2D sample. (*a*) Spectra taken at $k_{\|} = 0$ for increasing pumping power, the inset shows the integrated intensities. Angle-resolved spectra taken (*b*) below and (*c*) above threshold: the insets show the corresponding real space images of the emission. Reprinted with permission from [59]. Copyright 2009 American Institute of Physics.

have strong coupling, there must be a good spatial overlap between the photonic mode and the QWs, which must all be placed where the photonic field has a relative antinode. Increasing the density of injectable polaritons entails a further advantage in terms of a new relaxation mechanism: polaritons have a strong repulsive interaction, due to dipole and exchange terms between their excitonic parts [22, 56, 57], and can relax by elastic scattering with each other. Polariton–polariton scattering is a quadratic process in the pump power and has been shown to be the most efficient relaxation mechanism for polariton densities above 10^9 cm^{-2}.

Polariton lasing was firstly experimentally observed in a planar microcavity based on CdTe [40]. Kasprzak and co-workers showed the build up of a coherent polariton population in the energy minimum at $\boldsymbol{k}_{\|} = 0$. To further confirm the onset of a coherent state, they showed that the temporal coherence of the polariton laser becomes longer than the lifetime of a single polariton; this is a sign that a collective polariton state is formed, in which every polariton that decays radiatively is compensated by another scattering towards the lasing state and taking the same phase as the laser. They also showed, by spatially resolved interferometric measurements, an increase in the spatial coherence of the emission, which becomes much larger than the spatial coherence of a single polariton below threshold.

Polariton lasing was then also observed in GaAs samples. The most used design for polariton lasing in GaAs is that described in [58]: it consists of a half-wavelength AlAs cavity surrounded by two $Ga_{0.05}$ $Al_{0.95}As/Ga_{0.80}$ $Al_{0.20}$ As Bragg mirrors with 26 and 30 pairs in the top and bottom mirrors, respectively (the top has less pairs because of the larger refractive index contrasts with air with respect to the substrate). Three sets of four 7 nm GaAs QWs are inserted at the antinodes of the cavity mode electromagnetic field: one set is located at the centre of the cavity layer and the two others at the first antinode in each mirror. The sample has a Rabi splitting of 19 meV and the large number of pairs in the mirrors yields cavity mode lifetimes of several picoseconds.

An instance of polariton lasing in such a sample is shown in figure 5 (data are taken from [59]). Figure 5 shows spectra taken at $k_{\|} = 0$ for increasing pump powers, and their integrated intensities in the inset. The emitted intensity shows a clear lasing threshold after an initial linear increase. Care must be taken in these experiments to verify that lasing indeed occurs in strong coupling and the sample is not simply behaving as a VCSEL [60, 61]: the authors of [59] have chosen to study the emission pattern from the sample below (figure 5(*b*)) and above (figure 5(*c*)) threshold: in both cases the dispersion of the emission closely follows the expected curve for the lower polariton branch, and is far from the photon dispersion that the sample would display in weak coupling [61] (show by the line marked as C in the figure): the dispersion unambiguously proves that the sample is strong coupling while lasing.

5. The advantages of confinement

Lateral confinement is a technique well known in laser physics, and in particular in the case of VCSELS [31], to reduce the lasing threshold. The observation of polariton lasing in two-dimensional structures hinted at the realization of polaritons 'boxes', in which polaritons are confined in all three space directions. One obvious way to confine polaritons is to laterally pattern an optical microcavity in shape of pillars: this can be achieved by etching the microcavity through reactive ion etching after the pattern is written on the surface by means of electron beam lithography. The Bragg mirrors provide confinement of the photonic modes along the growth direction z, while the high index contrast between the semiconductor material (for instance $n = 3.45$ for GaAs) and air grants that the modes are confined along the other two directions. The QW is etched with the pillar, so that the exciton is naturally

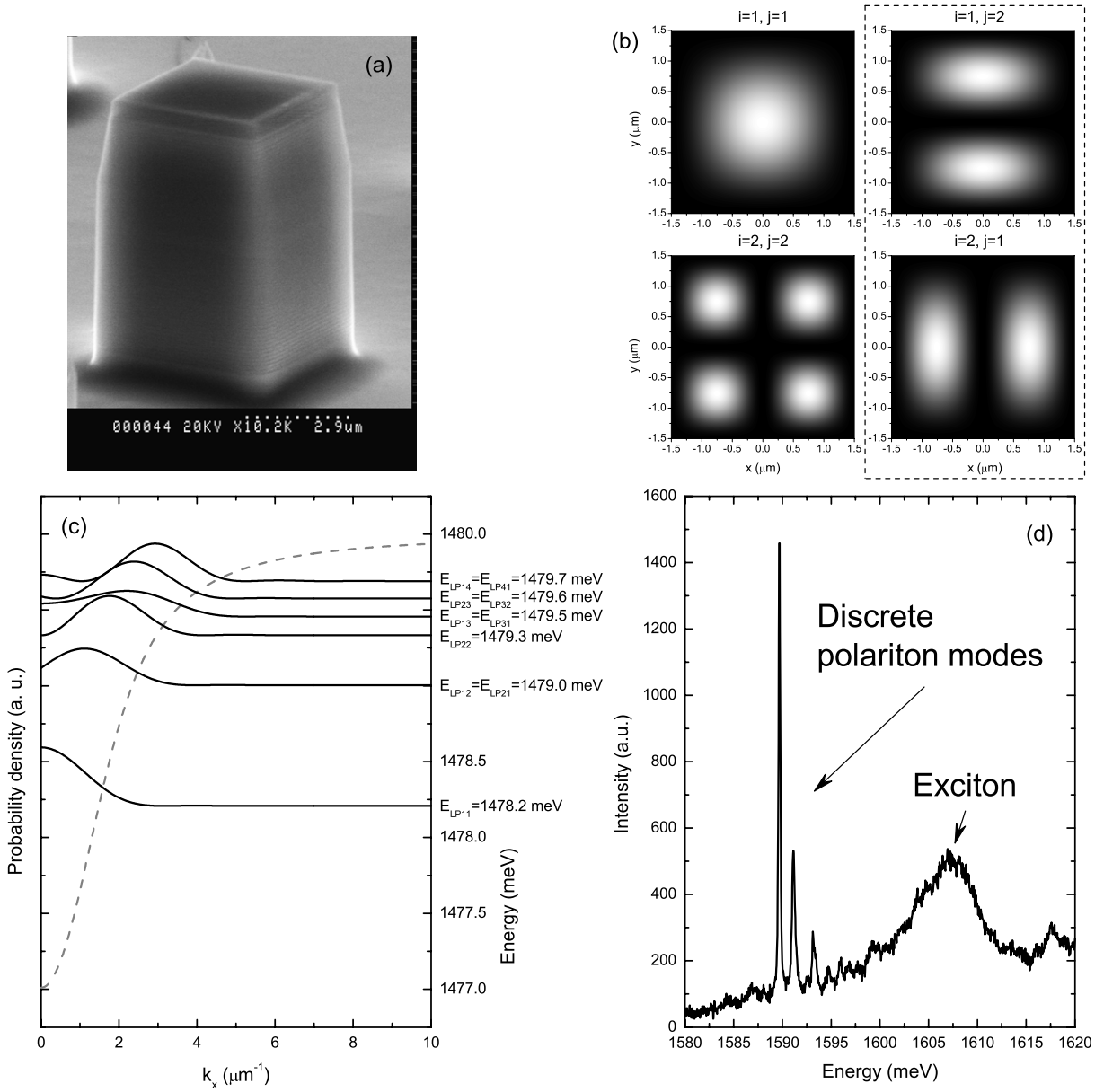

Figure 6. (*a*) SEM image of a micropillar cavity with side l =3 μm. (*b*) The square modulus of the field of the four modes with lowest energy of a micropillar with side $l = 3\,\mu$m following equations (14); the indexes i and j are the same as in equations (13) and (14). The mode with $i = 1$ and $j = 2$ has the same energy as the mode with $i = 2$ and $j = 1$ and their squared wavefunctions are enclosed within the dashed rectangle in the figure. (*c*) Grey dashed line, scale to the right: lower polariton dispersion for a GaAs-based microcavity with zero detuning and 8 meV Rabi splitting. Black lines, scale to the left: the square modulus of the fields in phase space along one of the pillar's sides, calculated taking the Fourier Transform of equation (14), for the same cavity as before once patterned in 3 μm pillars. The black curves were vertically shifted so that their bases correspond to the respective modal energy in the right scale, so that their distribution in phase space can be compared with the 2D dispersion (grey dashed line). (*d*) An example of photoluminescence from a 3 μm pillar GaAs-based pillar, clearly showing the exciton emission and discrete polariton states. Experiment performed with the sample at $T = 10$ K.

confined within it. An example of pillar etched in a GaAs microcavity is shown in figure 6(*a*).

Let us consider a square pillar of lateral size l. Equation (2) must now be implemented bearing in mind that the photon is confined along all directions. Along the growth direction k_z remains the same as in the planar cavity: $k_z = \frac{2\pi}{L_{\rm cav}}$. Along x and y, we can approximate the interface with air as a perfect mirror (this is a good approximation for pillars with size of several micrometres [62–65]), so that $k_x = \frac{2m_i\pi}{l}$ and $k_y = \frac{2m_j\pi}{l}$, where m_i and m_j are integer numbers. All three components of the wavevector are now quantized: this leads to discrete energy levels given by

$$E_{C,ij} = \frac{hc\boldsymbol{k}}{n} = \frac{hc}{n}\sqrt{\left(\frac{2\pi}{L_{\rm cav}}\right)^2 + \left(\frac{2m_i\pi}{l}\right)^2 + \left(\frac{2m_j\pi}{l}\right)^2}. \tag{13}$$

The corresponding photon wavefunctions are given by [62]

$$\langle \boldsymbol{x} \mid \psi_{i,j}\rangle = \sin\left(\frac{2m_i\pi}{l}x\right)\sin\left(\frac{2m_j\pi}{l}y\right)\phi\,(z) \tag{14}$$

where we have taken the origin to be on one of the square's angles and $\phi(z)$ is the electric field profile along the growth direction for a two-dimensional microcavity. An example for the three lower states in a square micropillar is shown in figure 6(*b*). Each photonic mode couples to the QW excitons independently through the Hamiltonian of equation (4) giving rise to multiple discrete polariton states (one lower polariton and one upper polariton for each discrete photon mode). The spatial profile of the polariton wavefunctions is still described by the wavefunctions of equation (14), as each photon mode couples with an exciton wavefunction having the same spatial profile [63].

One example is shown in figure 6(*c*) for the lower polaritons of a pillar of lateral size $l = 3\,\mu$m. The energy states are quantized forming a discrete ladder from the exciton states down to the fundamental level. Note that the model 14 is extremely simplified, and a correct calculation would need a complete numerical solution for the Maxwell equations using methods such as finite different time domain [66, 67] or plane wave expansion [68]. It is, however, interesting to consider the profile of the wavefunctions in phase space, plotted along one direction in figure 6(*c*): there is always an overlap between two functions of adjacent energy. This is a direct consequence of confinement: the lack of translational invariance along all direction implies that the wavevector $\boldsymbol{k}$ is no longer a good quantum number. This in turn means that the wavevector conditions on phonon relaxation in equations (12) are dropped: polaritons in micropillars can relax by emitting phonons with almost arbitrary $\boldsymbol{k}$, and thus confinement considerably helps polariton thermalization and lasing. An instance of photoluminescence spectrum taken on a square pillar with side $l = 3\,\mu$m is shown in figure 6(*d*). There are several discrete modes visible to the lower side of the exciton emission at 1607 meV. The discrete modes have a very high quality factors of the order of ten thousand.

The first thing to ascertain when patterning a microcavity is that pillars are in the strong coupling regime. Figure 7 shows the energies of the emitted modes for a series of pillars with $l = 4\,\mu$m: the pillars have different detuning with respect to the exciton but are otherwise identical[4]. A clear anti-crossing is visible, proof of strong coupling: the measured modes fit very well using the energies of equation (13) in strong coupling with the exciton with a Rabi splitting of 15 meV. The upper polariton modes are not visible in photoluminescence: their energy is several tens of meV above the fundamental states while the temperature corresponds to an energy of about 0.9 meV, and therefore the upper polariton states are almost completely depopulated.

Emission from a pillar of side $l = 6\,\mu$m is shown in figure 8 when increasing the pumping power P. The integrated emission data taken from figure 8 along with the energy of the main peak and its linewidth as a function of the pump power are reported in figure 9. The spectra at low power show

[4] Microcavities can easily be grown with the cavity layer being slightly wedged, so that the photon mode energy, and therefore the detuning depends on the position on the sample. If such a sample is patterned to obtain pillars, pillars in different positions on the wafer have different cavity thicknesses and so different detunings with respect to the exciton line.

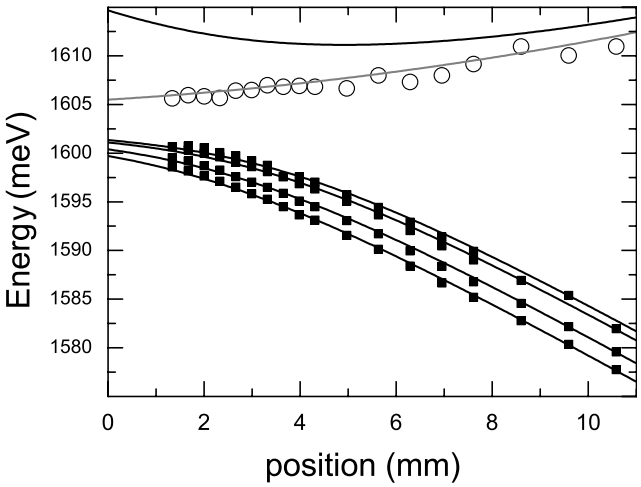

Figure 7. Emission energy of the discrete polariton lines (closed circles) and of the exciton line (open circles) measured on several 4 μm diameter micropillars varying the position on the wafer, (thick black lines) calculated energy of the 0D polariton modes. Data taken from [70], experiments performed at $T = 10$ K.

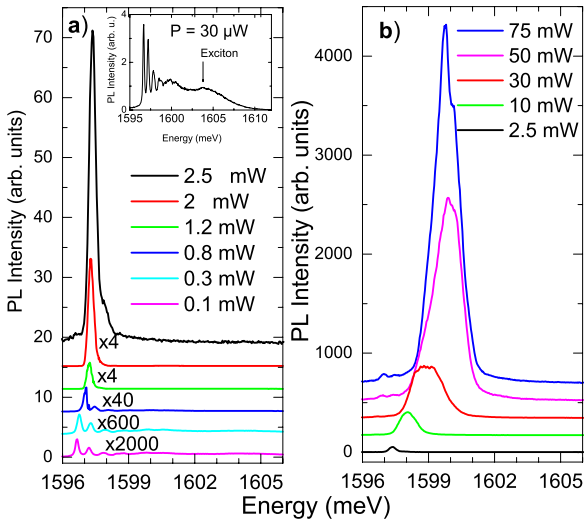

Figure 8. Emission spectra measured for several excitation powers in a single 6 μm diameter micropillar. (*a*) corresponds to the polariton lasing regime; spectra in (*b*) correspond to the loss of the strong coupling regime and the onset of photon lasing. Data taken from [70], experiments performed at $T = 10$ K.

emission from several discrete polariton states that initially increase linearly in intensity with the pump power. When the pump reaches 1 mW, there is, however, a steep superlinear increase in intensity for the fundamental mode, while the others disappear. The strong amplification of the emission is typical of a lasing threshold and is followed by a linear increase for about one order of magnitude in pumping power. During this second linear regime the emission undergoes a steep blueshift and significantly broadens: this is due to the occurrence of the Mott transition, in which the strong coupling is gradually lost and the emission gradually shifts towards the energy of the uncoupled photonic mode. Eventually the conduction and valence bands are filled and, with gain, a second lasing threshold is observed, this time in weak coupling, around $P = 45$ mW. This double threshold behaviour is typical of

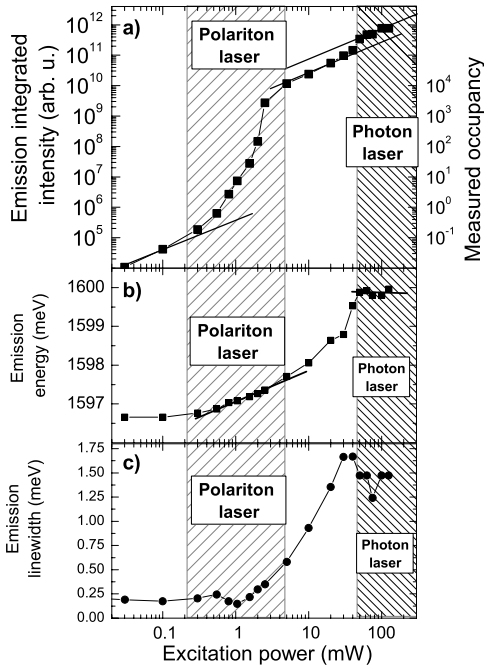

Figure 9. (*a*) Integrated intensity and measured occupancy , (*b*) emission energy and (*c*) emission linewidth measured on the lowest energy emission line of figure 8 as a function of the excitation power; dashed areas highlight the excitation range for polariton lasing or photon lasing. Data taken from [70], experiments performed at $T = 10\,\mathrm{K}$.

samples displaying both strong and weak coupling: at low powers, lasing of polariton is observed, without population inversion in the sample, and then at higher powers normal photon lasing is observed.

The ability to observe lasing in both strong and weak coupling in the same sample yields the possibility to clearly reveal the characteristics of polariton lasing and its peculiarities with respect to normal photon laser [70, 71]. The first clear difference is that the polariton emission line continuously blueshift. While at higher powers the blueshift is due to the loss of strong coupling, at low powers (even below threshold) the blueshift is linked to the excitonic part of polaritons. The polariton gas can strongly interact with itself and with the excitons in the reservoir and both these interactions are repulsive, with the effect of increasing the energy of the polariton gas when the system is more populated. The respective role of these two terms in the blueshift has been investigated in two-, one- and zero-dimensional polariton structures by the authors of [69].

Another peculiar behaviour of polariton lasers is the evolution of their linewidth. As long as heating effects can be neglected, in a conventional photon laser the linewidth δE decreases continuously following the law of Schawlow–Townes: $\frac{\delta E}{E_0} = \frac{1}{1+\langle N_{\mathrm{ph}}\rangle}$ where E_0 is the emission energy at threshold and $\langle N_{\mathrm{ph}}\rangle$ is the mean photon occupation. As shown in figure 9, in a polariton laser the linewidth decreases at threshold but then starts increasing again: this effect is due to the emission blueshift, and small instabilities in the pumping power (or, even in the case of a perfect pump, its shot noise) change the emission energy and thus, once averaged, the emission linewidth.

The fact of having discrete polariton states in micropillars is particularly advantageous to study polariton occupation of the levels. The mean occupation of the states can be experimentally assessed by measuring the output power I from the polariton laser, which means knowing the number of photons emitted from the sample which in turn are directly related to the polariton population via its radiative decay time τ_{rad} so that

$$\langle N\rangle = \frac{I}{\hbar\omega}\tau_{\mathrm{rad}} \tag{15}$$

where $\hbar\omega$ is the emission energy and τ_{rad} is obtained from the linewidth. The measured polariton population is shown in the right scale of figure 9(*a*) (limited to the strong coupling regime). As expected, the polariton lasing threshold occurs when the mean occupancy is around unity and bosonic stimulation begins. A total population of up to several thousands is observed in the sample before the strong coupling regime is lost, a sign that coherent macroscopic populations of quasi-particles can be maintained in solid-state samples. The ability to measure the actual polariton population in discrete states has been used to discern whether polariton lasers reach thermal equilibrium (i.e. whether they are 'standard' thermalized Bose–Einstein condensates); while the observation of a coherent macroscopic population of polaritons in the fundamental state, as shown in figure 7, would seem to point in that direction, it has been shown [70, 72] that, in the same pillar, polariton lasing can be obtained on different modes (and even on several modes at the same time), by simply changing the excitation conditions. Thermalized Bose–Einstein condensation necessarily occurs on the fundamental level [37] (energy levels below the condensate would otherwise need to have negative populations), so the experiments reported in [70] clearly show that polariton lasing is an out of equilibrium phenomenon.

The many advantages of micropillars come at the price of a technological difficulty in their fabrication. Etching a GaAs QW does in fact introduce a very fast nonradiative recombination channel for excitons at the surface, resulting in excitons too broad to obtain the strong coupling regime. The problem can be overcome by passivating the surface through chemical deposition: in the case of [70], the pillars were passivated by deposition of a thin layer of silica during the etching process. Several other geometries have been studied to confine polaritons in microcavities without the need of etching the QW, and polariton lasing has been observed in mechanical traps, which acts as a confining potential on the excitonic part of polaritons [41] and mesa structures, in which the thickness of the cavity layer is locally increased to confine polaritons through their photonic parts [73–78]. The disadvantage of these approaches is that the confining potential is weak (of the order of a few meVs) so that the effective volume of the confined modes is much larger than in the case of micropillars. Other approaches have been proposed which use only one Bragg mirror and confine polaritons using Tamm states [79–81] or Bloch surface waves [82–84], but have not yet been experimentally realized at the time of writing.

The most efficient way to confine polaritons in transparent materials is to use photonic crystals [85]. Photonic crystals

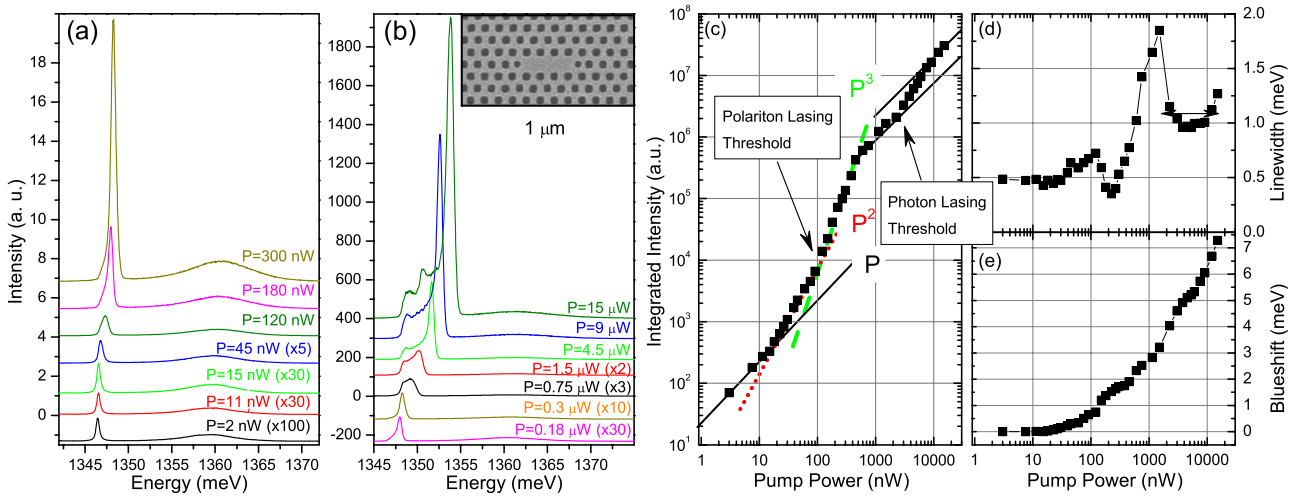

Figure 10. Photoluminescence spectra spectra taken in the regime of polariton lasing (*a*) and photon lasing (*b*) for a L3 cavity sample. The inset shows a scanning electron microscope picture of the cavity region. (*c*) Integrated intensity versus pump power, (*d*) linewidth and (e) blueshift versus pump power for the same sample. In (*c*), the continuous (black) line, the dotted (red) line and the dashed (green) line are a guide to the eye proportional to P, P^2 and P^3. Experiments performed at $T = 10$ K. Reprinted with permission from [109]. Copyright 2011, American Institute of Physics.

[86] are the two-dimensional analogue of Bragg stacks obtained by periodically modulating the refractive index of a planar waveguide (two-dimensional photonic crystals) usually by patterning it with periodic arrays of holes; this is achieved using a variety of top–down and bottom–up approaches [87–92]. Photonic crystals are a widely used tool in solid-state physics because they allow us to easily engineer the dispersion [93, 94] of the photonic bands by changing the sample design [95, 96].

Photonic crystals can be used to confine electromagnetic modes by the introduction of linear defects, acting as waveguides [97–101], and point defects acting as cavities [102]. Planar photonic crystal cavities have become a fundamental tool in modern photonics research, either for investigating basic cavity quantum electrodynamics effects [103, 104] and to demonstrate ultra-low threshold lasing [105]. One key feature of such nanocavities is the figure of merit represented by the ratio $Q/V_{\rm eff}$ between the cavity mode quality factor and its effective confinement volume. Modal volumes of the order of the cube of electromagnetic wavelength in the material can be achieved by the use of the L3 type cavity [102] obtained by removing a set of three holes by a triangle lattice of air holes in a semiconductor. The problem limiting the use of photonic crystals for polariton confinement still comes from non-radiative recombination of excitons caused by lateral patterning to obtain the photonic lattice. In GaAs photonic crystals, surface passivation is very difficult to obtain [106] and a solution has been found, for both interband [107] and intersubband [108], by periodically modulating the exponential tail of the photonic part of the polaritons confined in the planar waveguide. Such structures are, however, incompatible with the realization of cavities.

Polariton lasing has been recently reported [109] in L3 photonic crystal cavities by the use of InP-based materials, instead of GaAs-based materials, as the former suffer from negligible nonradiative recombination issues, even after patterning. The authors have reported quality factors of the order of 3000, while the modal volumes are a fraction of μm^3. An example of polariton lasing in InP photonic crystal cavities is in figure 10. The general behaviour is largely equivalent to the observations reported for micropillars; a double threshold is observed, as reported in the spectra in figures 10(*a*) and (*b*) and in the integrated intensities in figure 10(*c*). The same pattern for linewidth (figure 10(*d*)) and blueshift (figure 10(*e*)) is also observed, with the line narrowing at both thresholds, and the blueshift of the order of one meV at the first threshold and then increasing before the second threshold as the strong coping regime is gradually lost. The evident difference with the case of micropillars consists in the reduction of the polariton lasing threshold by more than three orders of magnitude. This reduction is due to the confining properties of the photonic crystal cavity: higher confinement implies higher density of states for the final state and therefore improved scattering towards the minimum in energy. The measured threshold of about 100 nW for the polariton laser is comparable to the lowest threshold reported to date for quantum dot lasers [105].

6. Polariton lasing at room temperature

One of the main limitations hindering the adoption of polariton-based effects in actual photonic devices is the fact that in GaAs-, InP- and CdTe-based samples polariton lasing can be observed only at low temperatures, requiring the use of cumbersome set-ups in which the samples are kept thermal contact with baths of liquid helium in the confines of cryostats. This limitation has physical origins: if we consider GaAs-based QWs, the exciton binding energy is of the order of 5–10 meVs, meaning that most excitons would be ionized for $T > 100$ K [110, 111]. To observe polaritonic effects at room temperature the choice must fall on different materials. In particular, gallium nitride-based QWs display excitons with binding energies of the order of 30 meV, while in zinc

oxide the exciton binding energy is of the order of 60 meV. Both GaN and ZnO, in their stable form, have a wurtzite crystal lattice, as opposed to the zinblende stucture of GaAs. In both materials excitons show extremely high oscillator strengths [112, 113].

The last decade has seen a very fast development of growth and technology of GaN-based devices, which has led to the development and industrial production of LEDs and lasers emitting in the blue and near ultraviolet ranges. Polariton devices must, however, meet very demanding specifications, requiring high quality factor photonic cavities to achieve the reversible interaction between excitons and photon fields necessary for the strong coupling regime. The main issue arising when trying to realize microcavities for strong coupling in GaN is related to its wurtzite crystalline structure: it is very difficult to grow planar Bragg mirrors with a large number of periods, as the strong lattice mismatch between GaN-based alloys easily causes the samples to crack. The solution adopted to overcome the problem is to limit the number of layers made of nitride alloys by growing half-cavities, where only the lower mirror is realized in GaN-based materials. The samples are then capped, *ex situ* by chemical vapour deposition, with a SiO_2-based upper Bragg mirror, to obtain a full microcavity sample. Microcavities with quality factors of some hundreds to a few thousands can be obtained with this method: while the Q-factor is lower than in the case of GaAs-based samples, nitride samples have excitons with higher oscillator strength, as discussed below, so that the observation of strong coupling is still possible.

The second problem related to the Wurtzite lattice is that heterojunctions, and in particular QWs, are plagued by extremely strong piezoelectric fields, which can broaden the QW exciton by the quantum confined Stark effect [114]. The electric field also has the effect of lowering the exciton oscillator strength, by pulling apart the electron and hole wavefunctions inside the QW. These effects can be mitigated by choosing the appropriate size of the QW, as described in [115][5] and [116].

Figure 11 shows an instance of a GaN microcavity sample. The transmission electron microscope image was taken on the half cavity, before the deposition of the top mirror, and shows good uniformity of the sample and the absence of cracks. The evidence of the occurrence of strong coupling in nitride samples was shown at first for bulk excitons in samples with no QWs [115, 117], and then for multiple QW samples [115] (see footnote 5): Rabi splitting of up to 50 meV was observed, corresponding to an oscillator strength an order of magnitude greater than in the case of GaAs-based QW excitons. The observation of strong coupling is performed, as usual, via angle-resolved experiments. An instance is shown in figure 12: angle-resolved reflectance is reported for a structure similar to that shown in figure 11. The experimental data show clear anticrossing, and the energies are well fitted by a strong coupling model as in equations (5). Room temperature polariton lasing in the sample is evidenced by studying the variation of photoluminescence with pump power, as shown in figure 13 [118, 119]. For powers below 20 W cm^{-2} the emission increases linearly with the pump, while above that value sharp changes in the emission are observed with all the characteristics of a polariton lasing threshold: steep superlinear increase in intensity, line narrowing and blueshift. Only one threshold was observed in the sample, and to show that lasing is indeed in strong coupling the author chose to study the emission pattern below and above the threshold: angle-resolved photoluminescence spectra are shown in figure 13. Below the threshold the emission is distributed along a large portion of the lower polariton branch; above the threshold a sharp lasing mode appears at $k_{\parallel} = 0$ at almost the same energy the emission had below the threshold, and far from the energy expected for weak coupling (the weak coupling of the exciton and the cavity mode are shown as dotted lines in the figure): this observation proves that the lasing emission occurs in strong coupling, and is therefore lasing of polaritons.

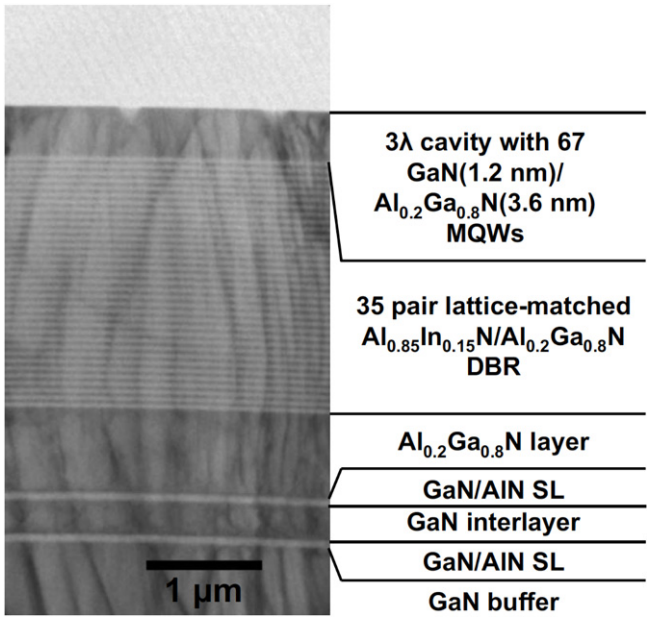

Figure 11. SEM Image of a GaN-based microcavity sample, with only the lower Bragg mirror (image taken before the deposition of the SiO_2-based upper Bragg mirror). Reprinted figure with permission from [115] (see footnote 5). Copyright 2008 by the American Physical Society.

In the case of ZnO, strong coupling has been observed in nanowires [120], microrods [121] and hybrid microcavities [122, 123]: polariton lasing has been reported only recently [124], due to the difficulties of growing samples with sufficiently high quality factor. Strong coupling at room temperature has also been observed in organic semiconductors with a variety of different compounds [125–127]. The difficulty of observing lasing in these samples comes from the fact than organic semiconductors undergo photobleaching processing at high pumping powers: polariton lasing in an organic samples was recently reported using an anthracene monocrystal as an active layer [128].

[5] Readers may view, browse, and or download material reprinted in this article from the above paper for temporary copying purposes only, provided these uses are for noncommercial personal purposes. Except as provided by law, this material may not be further reproduced, distributed, transmitted, modified, adapted, performed, displayed, published, or sold in whole or part, without prior written permission from the American Physical Society.

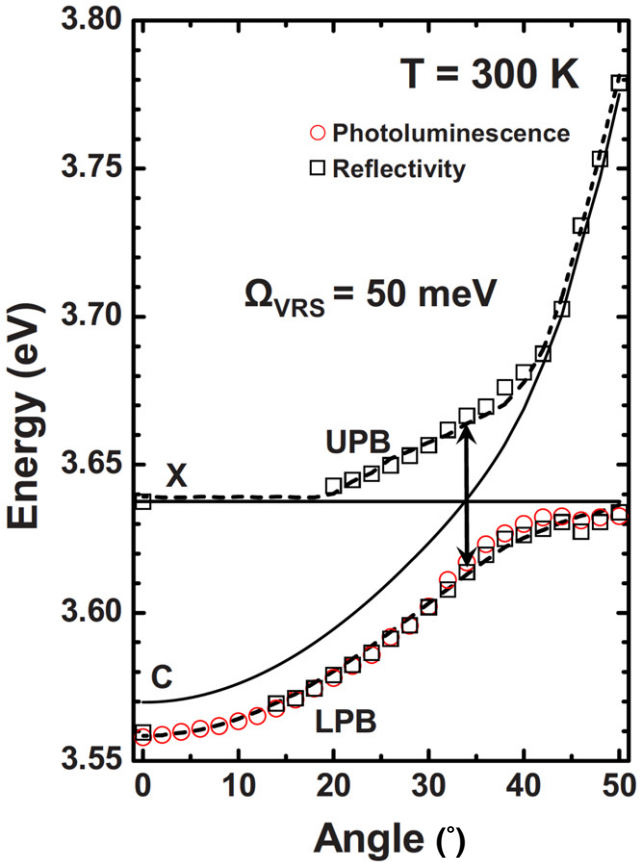

Figure 12. Experimental dispersion curves of a GaN microcavity sample deduced from angle resolved reflectivity spectra (empty squares) and photoluminescence spectra (empty red circles) and fits of the lower polariton band and the upper polariton band (dashed lines). The cavity mode C and the uncoupled exciton X are also reported (black lines). The data show a clear anticrossing, a sign that the sample is in strong coupling. Reprinted figures with permission from [115] (see footnote 5). Copyright 2008 by the American Physical Society.

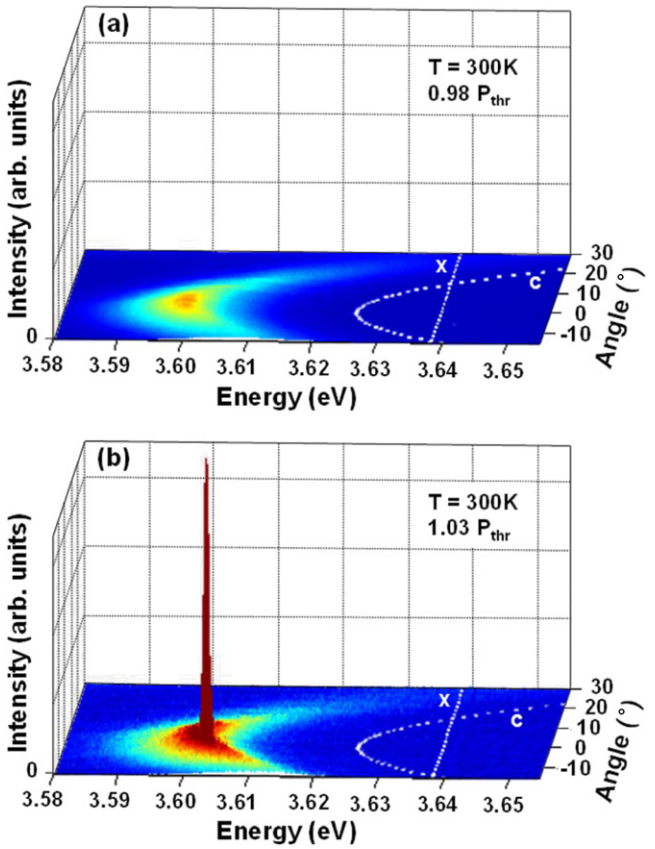

Figure 13. An example of polariton lasing at room temperature in a GaN-based sample: (*a*) emission pattern below threshold, and above threshold (*b*). Reprinted with permission from [119]. Copyright 2009, American Institute of Physics.

7. Conclusions

In this review we have tried to introduce the reader to the concept of polariton laser and some of the main results in the field. This introduction is far from being exhaustive: the reader can find a comprehensive description of strong coupling phenomena in semiconductor microcavities in the two books on polariton physics coauthored by Alexey Kavokin [129, 130] or the book Benoit Deveaud Pledran [131]. A review of more recent developments can be found in the collection of papers edited by Timofeev and Sanvitto [132]. For the problems related to polariton lasing at room temperature in GaN a review paper was recently published [133]. A review on polariton devices has also recently been published [134].

One obvious development for polariton lasers would be their integration in a structure suitable for current injection, so as to have a self-contained device in which no external pump is necessary. The interaction of polaritons in electric fields has already been reported in samples with doped Bragg mirrors [135–137] and electrical injection of polaritons has been recently shown [138–142]. For instance, the luminescence spectra shown in figures 2(*b*) and (*c*) are electroluminescence spectra taken with electrical injection of polaritons [138]. Nonetheless the observation of polariton lasing under electrical injection remains elusive and has not been reported to date. In the GaAs sample the problem lies in the high resistivity of the doped Bragg mirror, which results in Joule heating of the sample above the temperature at which polariton lasing is observable: completely different injection designs would be needed to overcome these problems. The hurdles associated with electrical injection of polaritons in large bandgap semiconductors are comprehensively treated in [133].

Some of the most interesting properties of polariton lasers are linked to their matter part. For instance, resonantly injected polaritons can behave as a superfluid [143, 144]: superfluidity has also been recently reported for non-resonantly injected polariton lasers [69]. Exciton polaritons have a well-defined spin, and their excitonic part yields a strong spin–spin interaction: this interaction has been used to propose several spin-based polariton devices [79, 80, 134, 147, 148], including polariton all-optical logic gates and polariton neurons [134]. Recently, polariton lasers have also been proposed as efficient terahertz emitters [147]. Polaritons have also attracted interest for their ultrafast switching capabilities [148–150]. Polariton lasers bear many characteristics in common with atomic condensates (see section 3.1) and, working at relatively high temperatures and in the solid state, they constitute an excellent

platform to study effects related to the physics of quantum gases, including quantum phase transitions and quantized vortices [151–155].

We have seen that one of the peculiarities of polariton lasers is their self-repulsion, resulting in a blueshift increasing with the population of polaritons. This property has been used to demonstrate extremely high optical nonlinearities under resonant injection [156–166], and has interesting consequences even below threshold: it has been proposed as a way to achieve optical nonlinearities at the single photon level [167]. When polariton lasers are concerned, it has been recently shown by Wertz *et al* [168] that this repulsive interaction can be exploited to exact a pushing force on polariton lasers: this result, coupled with the coherence properties and superfluid behaviour of polariton lasers, holds the promise of on-chip logical computation in a polaritonic environment.

Acknowledgments

The author thanks Jacqueline Bloch and Dario Gerace for careful reading of the manuscript. This work was supported by the foundation Alma Mater Ticinensis, by CNISM funding through the INNESCO project PcPol and by MIUR funding through the FIRB 'Futuro in Ricerca' project RBFR08XMVY.

References

[1] Purcell E M 1946 *Phys. Rev.* **69** 681
[2] Cohen-Tannoudji C, Diu B, Laloe F 2006 *Quantum Mechanics* (New York: Wiley-Interscience)
[3] Rabi I I 1937 *Phys. Rev.* **51** 652
[4] Thompson R J, Rempe G and Kimble J H 1992 *Phys. Rev. Lett.* **68** 1132
[5] Wallraff A, Schuster D I, Blais A, Frunzio L, Huang R S, Majer J, Kumar S, Girvin S M and Schoelkopf R J 2004 *Nature* **431** 162
[6] Yoshie T, Scherer A, Hendrickson J, Khitrova G, Gibbs H M, Rupper G, Ell C, Shchekin O B and Deppe D G 2004 *Nature* **432** 200
[7] Reithmaier J P *et al* 2004 *Nature* **432** 197
[8] Peter E, Senellart O, Martrou D, Lemaître A, Hours J, Gérard J M and Bloch J 2005 *Phys. Rev. Lett.* **95** 067401
[9] Weisbuch C, Nishioka M, Ishikawa A and Arakawa Y 1992 *Phys. Rev. Lett.* **69** 3314
[10] Bassani F, Tassone F and Andreani L C 1993 Excitons and polaritons in quantum wells, in Semiconductor Superlattices and Interfaces *Proc. International School of Physics 'E. Fermi', CXVII Course* ed A Stella (Amsterdam: North-Holland)
[11] Bastard G 1991 *Wave Mechanics Applied to Semiconductor Heterostructures* (New York: Wiley-Interscience)
[12] Yariv A and Teh P 1984 *Optical Waves in Crystals* (New York: Wiley)
[13] Whittaker D M, Kinsler P, Fisher T A, Skolnick M S, Armitage A, Afshar A M and Roberts J S 1996 *Phys. Rev. Lett.* **77** 4792
[14] Andreani L C and Pasquarello A 1990 *Phys. Rev.* B **42** 8928
[15] Savona V, Andreani L C, Schwendimann P and Quattropani A 1995 *Solid State Commun.* **93** 733
[16] Andreani L C 2003 *Electron and Photon Confinement in Semiconductor Nanostructures* ed B Deveaud *et al* (Amsterdam: IOS Press) p 105
[17] Andreani L C, Tassone F and Bassani F 1991 *Solid State Commun.* **77** 641
[18] Sermage B, Deveaud-Pledran B, Berz M, Clerot F, Long S, Katzer D S and Mollot F 1993 *Proc. SPIE* **1985** 368
[19] Loudon R 2003 *The Quantum Theory of Light* (Oxford: Oxford University Press)
[20] Imamoglu A, Ram R J, Pau S and Yamamoto Y 1996 *Phys. Rev.* A **53** 4250
[21] Tassone F and Yamamoto Y 1999 *Phys. Rev.* B **59** 10830
[22] Tassone F, Piermarocchi C, Savona V, Quattropani A and Schwendimann P 1997 *Phys. Rev.* B **56** 7554
[23] Glauber R 2006 *Rev. Mod. Phys.* **78** 1267
[24] Laussy F P, Malpuech G, Kavokin A and Bigenwald P 2004 *Phys. Rev. Lett.* **93** 016402
[25] Kasprzak J, Richard M, Baas A, Deveaud-Pledran B, André Poizat J P and Le Si Dang D 2008 *Phys. Rev. Lett.* **100** 067402
[26] Aßmann M, Tempela J S, Veit F, Bayer M, Rahimi-Iman A, Löffler A, Höfling S, Reitzenstein S, Worschech L and Forchel A 2011 *Proc. Natl Acad. Sci.* **108** 1804
[27] Huang D, Chyi J and Morkoç H 1990 *Phys. Rev.* B **42** 5147
[28] Choi M, Je K, Yim S Y and Park S H 2004 *Phys. Rev.* B **70** 085309
[29] Houdré R, Gibernon J L, Pellandini P, Stanley R P, Oesterle U, Weisbuch C, Ogorman J, Roycroft B and Ilegems M 1995 *Phys. Rev.* B **52** 7810
[30] Kappei L, Szczytko J, Morier-Genoud F and Deveaud-Pledran B 2005 *Phys. Rev. Lett.* **94** 147403
[31] Sale T E 1995 *Vertical Cavity Surface Emitting Lasers* (Baldock, UK: Research Studies Press)
[32] Butov L V, Gossard A C and Chemla D S 2002 *Nature* **418** 751
[33] Butov L V, Lai C W, Ivanov A L, Gossard A C and Chemla D S 2002 *Nature* **417** 47
[34] Butov L V 2003 *Solid State Commun.* **127** 89
[35] High A A, Leonard J R, Hammack A T, Fogler M M, Butov L V, Kavokin A V, Campman K L and Gossard A C 2012 *Nature* **483** 584
[36] Yoshioka K, Chae E and Kuwata-Gonokami M 2011 *Nature Commun.* **2** 328
[37] Reif F 1965 *Statistical and Thermal Physics* (New York: McGraw-Hill)
[38] Malpuech G, Rubo Y G, Laussy F P, Bigenwald P and Kavokin A V 2003 *Semicond. Sci. Technol.* **18** S395
[39] Butte R, Levrat J, Christmann G, Feltin E, Carlin J F and Grandjean N 2010 *Phys. Rev.* B **80** 233301
[40] Kasprzak J *et al* 2006 *Nature* **443** 409
[41] Balili R, Hartwell V, Snoke D, Pfeiffer L and West K 2007 *Science* **316** 1007
[42] Richard M, Kasprzak J, Baas A, Lagoudakis K, Wouters M, Carusotto I, André R, Deveaud-Plédran B and Le Si Dang D 2010 *Int. J. Nanotechnol.* **7** 668
[43] Deveaud-Plédran B 2012 *J. Opt. Soc. Am.* B **29** A138
[44] Sarchi D and Savona V 2005 *Phys. Status Solidi* b **242** 2290
[45] Butov L V and Kavokin A V 2012 *Nature Photon.* **6** 2
[46] Deveaud-Plédran B 2012 *Nature Photon.* **6** 205
[47] Grosso G and Pastori Parravicini G 2000 *Solid State Physics* (London: Academic)
[48] Yamamoto Y, Tassone F and Cao H 2000 *Semiconductor Cavity Quantum Electrodynamics* (*Springer Tracts in Modern Physics* v 169) (Berlin: Springer)
[49] Senellart P, Bloch J, Sermage B and Marzin J Y 2000 *Phys. Rev.* B **62** R16263
[50] Tartakovskii A I, Emam-Ismail M, Stevenson R M, Skolnick M S, Astratov V N, Whittaker D M, Baumberg J J and Roberts J S 2000 *Phys. Rev.* B **62** R2283
[51] Müller M, Bleuse J and André R 2000 *Phys. Rev.* B **62** 16886
[52] Pau S, Björk P, Cao H, Tassone F, Huang R, Yamamoto Y and Stanley R P 1997 *Phys. Rev.* B **55** R1942

[53] Malpuech G, Kavokin A, Di Carlo A and Baumberg J J 2002 *Phys. Rev.* B **65** 153310
[54] Perrin M, Senellart P, Lemaître A and Bloch J 2005 *Phys. Rev.* B **72** 075340
[55] Bajoni D, Perrin M, Senellart P, Lemaître A, Sermage B and Bloch J 2006 *Phys. Rev.* B **73** 205344
[56] Ciuti C, Schwendimann P, Deveaud-Pledran B and Quattropani A 2000 *Phys. Rev.* B **62** R4825
[57] Senellart P and Bloch J 1999 *Phys. Rev. Lett* **82** 1233
[58] Bloch J, Freixanet T, Marzin J Y, Thierry-Mieg V and Planel R 1998 *Appl. Phys. Lett.* **73** 1694
[59] Wertz E, Ferrier L, Solnyshkov D D, Bajoni D, Miard A, Lemaître A, Malpuech G and Bloch J 2009 *Appl. Phys. Lett.* **95** 051108
[60] Bajoni D, Senellart P, Lemaître A and Bloch J 2007 *Phys. Rev.* B **76** 201305
[61] Butté R *et al* 2002 *Phys. Rev.* B **65** 205310
[62] Reithmaier J P, Röhner M, Zull H, Schäfer F, Forchel A, Knipp P A and Reinecke T L 1997 *Phys. Rev. Lett.* **78** 378
[63] Panzarini G and Andreani L C 1999 *Phys. Rev.* B **60** 16799
[64] Gérard J M, Barrier D, Marzin J Y, Kuszelewicz R, Manin L, Costard E, Thierry-Mieg V and Rivera T 1996 *Appl. Phys. Lett.* **69** 449
[65] Dasbach G, Schwab M, Bayer M and Forchel A 2001 *Phys. Rev.* B **64** 201309(R)
[66] Ho Y L D, Cao T, Ivanov P S, Cryan M J, Craddock I J, Railton C J and Rarity J G 2007 *IEEE J. Quantum Electron* **43** 462
[67] Xu Y, Vuckovic J, Lee R, Painter O, Scherer A and Yariv A 1999 *J. Opt. Soc. Am.* B **16** 465
[68] Liscidini M, Gerace D, Andreani L C and Sipe J E 2008 *Phys. Rev.* B **77** 035324
[69] Ferrier L, Wertz E, Johne R, Solnyshkov D D, Senellart P, Sagnes I, Lemaître A, Malpuech G and Bloch J 2011 *Phys. Rev. Lett* **106** 126401
[70] Bajoni D, Senellart P, Wertz E, Sagnes I, Miard A, Lemaître A and Bloch J 2008 *Phys. Rev. Lett.* **100** 047401
[71] Tsotsis P, Eldridge P S, Gao T, Tsintzos S I, Hatzopoulos Z and Savvidis P G 2012 *New J. Phys.* **14** 023060
[72] Bajoni D, Wertz E, Senellart P, Lemaître A, Bouchoule S and Bloch J 2008 *Acta Phys. Pol.* A **114** 933
[73] El Daïf O, Baas A, Guillet T, Brantut J P, Idrissi Kaitouni R, Staehli J L, Morier-Genoud F and Deveaud-Plédran B 2006 *Appl. Phys. Lett.* **88** 061105
[74] Lugan P, Sarchi D and Savona V 2006 *Physica Status Solidi* c **3** 2428
[75] Portolan S, Hauke P and Savona V 2008 *Physica Status Solidi* b **245** 1089
[76] Nardin G, Paraïso T K, Cerna R, Pietka B, Léger Y, El Daïf O, Morier-Genoud F and Deveaud-Plédran B 2009 *Appl. Phys. Lett.* **94** 181103
[77] Sanvitto D, Amo A, Vina L, André R, Solnyshkov D and Malpuech G 2009 *Phys. Rev.* B **80** 045301
[78] Manni F, Lagoudakis K G, Pietka B, Fontanesi F, Wouters M, Savona V, André R and Deveaud-Plédran B 2011 *Phys. Rev. Lett.* **106** 176401
[79] Liew T C H, Kavokin A V and Shelykh I A 2008 *Phys. Rev. Lett.* **101** 016402
[80] Liew T C H, Kavokin A V, Ostatnicky T, Kaliteevski M, Shelykh I A and Abram R A 2010 *Phys. Rev.* B **82** 033302
[81] Gazzano O, Vasconcellos S, Gauthron K, Symonds C, Bloch J, Voisin P, Bellessa J, Lemaître A and Senellart P 2011 *Phys. Rev. Lett.* **107** 247402
[82] Liscidini M, Galli M, Shi M, Dacarro G, Patrini M, Bajoni D and Sipe J E 2009 *Opt. Lett.* **34** 2318
[83] Liscidini M and Sipe J E 2009 *J. Opt. Soc. Am.* B **26** 279
[84] Liscidini M, Gerace D, Sanvitto D and Bajoni D 2011 *Appl. Phys. Lett.* **98** 121118
[85] Gerace D and Andreani L C 2007 *Phys. Rev.* B **75** 235325
[86] Joannopoulos J D, Johnson S G, Winn J N and Meade R D 2008 *Photonic Crystals: Molding the Flow of Light* (Princeton, NJ: Princeton University Press)
[87] Cheng C C and Scherer A 1995 *J. Vac. Sci. Technol.* B **13** 2696
[88] Braive R, Le Gratiet L, Guilet S, Patriarche G, Lemaître A, Beveratos A, Robert-Philip I and Sagnes I 2009 *J. Vac. Sci. Technol.* B **27** 1909
[89] Romanato F *et al* 2002 *Nanotechnology* **13** 644
[90] Romanato F, Cojoc D, Di Fabrizio E, Galli M and Bajoni D 2003 *J. Vac. Sci. Technol.* B **21** 2912
[91] Belotti M, Galli M, Bajoni D, Andreani L C, Guizzetti G, Decanini D and Chen Y 2003 *Microelectron. Eng.* **73–74** 405
[92] Pallavidino L *et al* 2006 *J. Non-Cryst. Solids* **352** 1425
[93] Galli M *et al* 2002 *Eur. Phys. J.* B **27** 79
[94] Andreani L C *et al* 2003 *Synth. Met.* **139** 695
[95] Galli M, Bajoni D, Marabelli F, Andreani L C, Pavesi L and Pucker G 2004 *Phys. Rev.* B **69** 115107
[96] Estephan E *et al* 2010 *Langmuir* **26** 10373
[97] Notomi M, Yamada K, Shinya A, Takahashi J, Takahashi C and Yokohama I 2001 *Phys. Rev. Lett.* **87** 253902
[98] Galli M, Belotti M, Bajoni D, Patrini M, Guizzetti G, Gerace D, Agio M, Andreani L C and Chen Y 2004 *Phys. Rev.* B **70** 081307
[99] Galli M *et al* 2005 *IEEE J. Sel. Areas Commun.* **23** 1402
[100] Galli M, Bajoni D, Patrini M, Guizzetti G, Gerace D, Andreani L C, Belotti M and Chen Y 2005 *Phys. Rev.* B **72** 125322
[101] Gerace D *et al* 2005 *Appl. Phys. Lett.* **87** 211116
[102] Akahane Y, Asano T, Song B S and Noda S 2003 *Nature* **425** 944
[103] Englund D, Fattal D, Waks E, Solomon G, Zhang B, Nakaoka T, Arakawa Y, Yamamoto Y and Vučković J 2005 *Phys. Rev. Lett.* **95** 013904
[104] Hennessy K, Badolato A, Winger M, Gerace D, Atatüre M, Gulde S, Fält S, Hu E and Imamoğlu A 2007 *Nature* **445** 896
[105] Strauf S, Hennessy K, Rakher M T, Choi Y S, Badolato A, Andreani L C, Hu E L, Petroff P M and Bouwmeester B 2006 *Phys. Rev. Lett* **96** 127404
[106] Englund D, Altug H, and Vuković J 2007 *Appl. Phys. Lett.* **91** 071124
[107] Bajoni D *et al* 2009 *Phys. Rev.* B **80** 201308(R)
[108] Zanotto S, Biasiol G, Degli Innocenti R, Sorba L and Tredicucci A 2010 *Appl. Phys. Lett.* **97** 231123
[109] Azzini S, Gerace D, Galli M, Sagnes I, Braive R, Lemaître A, Bloch J and Bajoni D 2011 *Appl. Phys. Lett* **99** 111106
[110] Phillips R T, Nixon G C, FujitaT, Simmons M Y, Ritchie D A 1996 *Solid State Commun.* **98** 287
[111] Saha M N 1921 *Proc. R. Soc. Lond.* **99** 135
[112] Gil B 2001 *Phys. Rev.* B **64** 201310(R)
[113] Zamfirescu M, Gil B, Grandjean N, Malpuech G, Kavokin A, Bigenwald P and Massies J 2001 *Phys. Rev.* B **64** 121304
[114] Leroux M, Grandjean N, Laügt M, Massies J, Gil B, Lefebvre P and Bigenwald P 1998 *Phys. Rev.* B **58** R13371
[115] Butté R, Christmann G, Feltin E, Carlin J F, Mosca M, Ilegems M and Grandjean N 2006 *Phys. Rev.* B **73** 033315
[116] Bernardini F, Fiorentini V and Vanderbilt D 1997 *Phys. Rev.* B **56** R10024
[117] Semond F, Sellers I R, Natali F, Byrne D, Leroux M, Massies J, Ollier N, Leymarie J, Disseix P and Vasson A 2005 *Appl. Phys. Lett.* **87** 021102
[118] Christopoulos S *et al* 2007 *Phys. Rev. Lett.* **98** 126405
[119] Christmann G, Butté R, Feltin E, Carlin J F and Grandjean N 2008 *Appl. Phys. Lett* **93** 051102
[120] Van Vugt L K, Rühle S, Ravindran P, Gerritsen H C, Kuipers L and Vanmaekelbergh D 2006 *Phys. Rev. Lett.* **97** 147401

[121] Sun L, Chen Z, Ren Q, Yu K, Bai L, Zhou W, Xiong H, Zhu H Q and Shen X 2008 *Phys. Rev. Lett* **100** 156403
[122] Guillet T, Brimont C, Valvin P, Gil B, Bretagnon T, Médard F, Mihailovic M, Zúniga-Pérez J, Leroux M, Semond F and Bouchoule S 2011 *Appl. Phys. Lett.* **98** 211105
[123] Shimada R, Xie J, Avrutin V, Özgür U and Morko c H 2008 *Appl. Phys. Lett.* **92** 011127
[124] Guillet T *et al.* 2011 *Appl. Phys. Lett.* **99** 161104
[125] Frezza L, Patrini M, Liscidini M and Comoretto D 2011 *J. Phys. Chem.* C **115** 19939
[126] Lidzey D G, Bradley D D C, Skolnick M S, Virgili T, Walker S and Whittaker D M 1998 *Nature* **395** 53
[127] Lanty G, Bréhier A, Parashkov R, Lauret J S and Deleporte E 2008 *New J. Phys.* **10** 065007
[128] Kéna-Cohen S and Forrest S R 2010 *Nature Photon.* **4** 371
[129] Kavokin A V and Malpuech G 2003 *Cavity Polaritons* (New York: Academic)
[130] Kavokin A V, Baumberg J J and Malpuech G 2007 *Microcavities* (Oxford: Oxford University Press)
[131] Deveaud-Plédran B 2006 *The Physics of Semiconductor Microcavities* (New York: Wiley VCH)
[132] Sanvitto D and Timofeev V 2012 *Title: Exciton Polaritons in Microcavities: New Frontiers* (*Springer Series in Solid-State Sciences*) (Berlin: Springer)
[133] Butté R and Grandjean N 2011 *Semicond. Sci. Technol.* **26** 014030
[134] Liew T C H, Shelykh I A and Malpuech G 2011 *Physica E* **43** 1543
[135] Fisher T A, Afshar A M, Skolnick M S, Whittaker D M, Roberts J S, Hill G and Pate M A 1996 *Solid State Electron.* **40** 493
[136] Bajoni D, Semenova E , Lemaitre A, Bouchoule S, Wertz E, Senellart P, Barbay S, Kuszelewicz R and Bloch J 2008 *Phys. Rev. Lett.* **101** 266402
[137] Bajoni D, Semenova E, Lemaître A, Barbay S, Kuszelewicz R and Bloch J 2010 *Appl. Phys. Lett.* **97** 091107
[138] Bajoni D, Semenova E, Lemaître A, Bouchoule S, Wertz E, Senellart P and Bloch J 2008 *Phys. Rev.* B **77** 113303
[139] Bajoni D, Miard A, Lemaître A, Bouchoule A, Bloch J and Tignon J 2007 *Appl. Phys. Lett.* **90** 121114
[140] Bajoni D, Miard A, Lemaître A, Bouchoule A, Bloch J and Tignon J 2007 *Superlatt. Microstruct.* **41** 368
[141] Khalifa A A, Love A P D, Krizhanovskii D N, Skolnick M S and Roberts J S 2008 *Appl. Phys. Lett.* **92** 061107
[142] Tsintzos S I, Pelekanos N T, Konstantinidis G, Hatzopoulos Z and Savvidis P G 2008 *Nature* **453** 372
[143] Amo A *et al* 2009 *Nature* **457** 291
[144] Amo A, Lefrére J, Pigeon S, Adrados C, Ciuti C, Carusotto I, Houdré R, Giacobino E and Bramati A 2009 *Nature Phys.* **5** 805
[145] Paraïso T K, Wouters M, Léger Y, Morier-Genoud F and Deveaud-Plédran B 2010 *Nature Mater.* **9** 655
[146] Amo A, Liew T C H, Adrados C, Houdré R, Giacobino E, Kavokin A V and Bramati A 2010 *Nature Photon.* **4** 361
[147] Kavokin A V, Shelykh I A, Taylor T and Glazov M M 2012 *Phys. Rev. Lett.* **108** 197401
[148] Scherbakov A V, Berstermann T, Akimov A V, Yakovlev D R, Beaudoin G, Bajoni D, Sagnes I, Bloch J and Bayer M 2008 *Phys. Rev.* B **78** 241302
[149] Amo A, Ballarini D, Sanvitto D, Kozhemyakina E, Viña L, Lemaître A, Bajoni D and Bloch J 2008 *Appl. Phys. Lett.* **92** 061912
[150] Amo A, Ballarini D, Sanvitto D, Kozhemyakina E, Viña L, Lemaître A, Bajoni D and Bloch J 2008 *Phys. Status Solidi* B **245** 1064
[151] Lagoudakis K G, Wouters M, Richard M, Baas A, Carusotto I, André R, Le Si Dang D and Deveaud-Plédran B 2008 *Nature Phys.* **4** 706
[152] Lagoudakis K G, Ostatnický T, Kavokin A V, Rubo Y G, André R and Deveaud-Plédran B 2009 *Science* **326** 974
[153] Sanvitto D *et al* 2010 *Nature Phys.* **6** 527
[154] Lagoudakis K G, Manni F, Pietka B, Wouters M, Liew T C H, Savona V, Kavokin A V, André R and Deveaud-Plédran B 2011 *Phys. Rev. Lett.* **106** 115301
[155] Manni F, Lagoudakis K G, Liew T C H, André R and Deveaud-Plédran B 2011 *Phys. Rev. Lett.* **107** 106401
[156] Savvidis P G, Baumberg J J, Stevenson R M, Skolnick M S, Whittaker D M and Roberts J S 2000 *Phys. Rev. Lett.* **84** 1547
[157] Stevenson R M, Astratov V, Skolnick M S, Whittaker D M, Emam-Ismail M, Tartakovskii A I, Savvidis P G, Baumberg J J and Roberts J S 2000 *Phys. Rev. Lett.* **85** 3680
[158] Saba M *et al* 2001 *Nature* **414** 731
[159] Diederichs C, Tignon J, Dasbach G, Ciuti C, Lemaître A, Bloch J, Roussignol P and Delalande P 2006 *Nature* **440** 904
[160] Portolan S, Di Stefano O, Savasta S and Savona V 2009 *Europhys. Lett.* **88** 20003
[161] Portolan S, Di Stefano O, Savasta S, Rossi F and Girlanda R 2008 *Phys. Rev.* B **77** 195305
[162] Portolan S, Di Stefano O, Savasta S, Rossi F and Girlanda R 2008 *Phys. Rev.* B **77** 035433
[163] Butté R, Skolnick M S, Whittaker D M, Bajoni D and Roberts J S 2003 *Phys. Rev.* B **68** 115325
[164] Bajoni D, Peter E, Senellart P, Smirr J L, Sagnes I, Lemaître A and Bloch J 2007 *Appl. Phys. Lett.* **90** 051107
[165] Bajoni D, Senellart P, Peter E, Smirr J L, Sagnes I, Lemaître A and Bloch J 2007 *AIP Conf. Proc.* **893** 1143
[166] Xie W, Dong H, Zhang S, Sun L, Zhou W, Ling Y, Lu J, Shen X and Chen Z 2012 *Phys. Rev. lett.* **108** 166401
[167] Verger A, Ciuti C and Carusotto I 2006 *Phys. Rev.* B **73** 193306
[168] Wertz E *et al* 2010 *Nature Phys.* **6** 860